Scilight

Sustainable Engineering Novit

https://www.sciltp.com/journals/sen

Review

Multiscale Simulation in Fuel Cell and Electrolyzer Systems: A Review of Methods, Applications, and Future Prospects

Kadi Hu [1], Bo Li [2,*], Ziqi Tian [1,*] and Liang Chen [1]

[1] Zhejiang Key Laboratory of Advanced Fuel Cells and Electrolyzers Technology, Ningbo Institute of Materials Technology and Engineering, Chinese Academy of Sciences, Ningbo 315201, China
[2] Department of Chemical and Biomolecular Engineering, Vanderbilt University, 2301 Vanderbilt Place, Nashville, TN 37235, USA
* Correspondence: bo.li.2@vanderbilt.edu (B.L.); tianziqi@nimte.ac.cn (Z.T.)

How To Cite: Hu, K.; Li, B.; Tian, Z.; et al. Multiscale Simulation in Fuel Cell and Electrolyzer Systems: A Review of Methods, Applications, and Future Prospects. *Sustainable Engineering Novit* **2025**, *1*(1), 5. https://doi.org/10.53941/sen.2025.100005

Received: 22 August 2025
Revised: 10 September 2025
Accepted: 28 September 2025
Published: 24 October 2025

Abstract: This review explores the transformative role of multiscale modeling in advancing fuel cell and electrolyzer technologies, which are essential for achieving decarbonized energy systems. By integrating quantum-level reaction mechanisms, mesoscale transport phenomena, and macroscopic system dynamics, it establishes a cohesive framework for optimizing electrochemical device performance. Key theoretical advances are discussed, including hybrid quantum-mechanics/continuum approaches that capture ionic interactions at atomic resolution, and machine learning-enhanced models that accurately predict microstructural evolution. The review highlights how AI-driven multiscale simulations simultaneously reduce computational demands and enhance predictive power, particularly in assessing material degradation and performance thresholds. Importantly, this work bridges the traditional divide between electrochemical modeling and data science, paving the way for digital twin technologies. By addressing challenges in scale coupling and model validation, this study accelerates the path toward commercial development of high-efficiency hydrogen technologies. These findings are especially relevant for industries pursuing net-zero targets through advanced energy storage solutions, providing both methodological innovations and practical guidance for next-generation fuel cell design.

Keywords: fuel cell; electrolyzer; multiscale simulation; machine learning; electrochemical interface

1. Introduction

Amidst the global push for decarbonization and sustainable energy solutions, hydrogen has emerged as a pivotal energy carrier for the future [1,2]. Fuel cells and electrolyzers stand out as cornerstone technologies within the burgeoning hydrogen economy [3–5]. Fuel cells, serving as cornerstone devices for zero-emission energy conversion, efficiently transform hydrogen's chemical energy into electricity and play a vital role in decarbonizing two critical sectors, i.e., heavy-duty transportation and stationary energy storage. However, achieving these performance benchmarks depends on overcoming cross-scale challenges. For instance, the power density of heavy-duty fuel cells is governed by atomic-scale oxygen reduction reaction (ORR) activity at catalytic sites as well as macroscopic reactant distribution within bipolar plate flow channels. At the same time, long-term durability requires careful monitoring of mesoscale degradation mechanisms, such as catalyst particle coarsening in electrodes. Complementing fuel cells, electrolyzers produce green hydrogen through renewable-powered water splitting. Yet their operational efficiency under variable solar and wind energy inputs hinges on the

Copyright: © 2025 by the authors. This is an open access article under the terms and conditions of the Creative Commons Attribution (CC BY) license (https://creativecommons.org/licenses/by/4.0/).
Publisher's Note: Scilight stays neutral with regard to jurisdictional claims in published maps and institutional affiliations.

synchronization of scale-dependent phenomena, including nanoscale bubble nucleation dynamics at electrode surfaces and macroscopic thermal-electrochemical coupling. These intricate cross-scale interactions, where atomic-level reactions, mesoscale transport, and macroscopic device design mutually constrain one another, highlighting the limitations of traditional single-scale modeling approaches and underscore the necessity of multiscale simulation techniques [6–9].

The complexity and multi-scale nature of electrochemical systems, including fuel cells and electrolyzers, pose significant challenges for their design and optimization. These systems encompass physical and chemical phenomena spanning vast ranges of length and time scales, from quantum-level electron transfer events to macroscopic device performance. Traditional single-scale modeling approaches are inherently limited in their ability to provide a comprehensive understanding of such complex systems. For instance, while macroscopic computational fluid dynamics (CFD) models effectively simulate phenomena like reactant transport and temperature distribution within flow channels, they fail to capture the key microscopic processes at the electrode/electrolyte interface. This limitation prevents them from explaining core questions, such as why slight adjustments to macroscopic flow field parameters can drastically alter catalytic efficiency. Conversely, purely quantum mechanics (QM) or molecular dynamics (MD) models can accurately calculate microscopic properties like reaction energy barriers and interfacial interaction energies. However, their prohibitive computational scale prevents them from connecting these insights to device-level macroscopic performance, thus offering limited guidance for the structural optimization of practical electrolyzers or fuel cells.

Hence, the emergence of multiscale modeling as a powerful paradigm that bridges different scales by systematically linking models operating at various levels of detail is paramount. Multiscale modeling not only facilitates a deeper understanding of the fundamental physics and chemistry governing these systems but also has the potential to significantly accelerate material discovery, optimize operational processes, and reduce product development time and costs [10–12]. Consequently, adapting and extending multiscale modeling to fuel cells and electrolyzers present unique challenges, including the accurate representation of interfaces, the efficient transfer of information across scales, and the computational costs associated with high-fidelity simulations [13–16]. This study aims to provide a comprehensive review of multiscale modeling methodologies, applications, and future prospects in fuel cell and electrolyzer systems. We will explore various modeling techniques employed at microscopic, mesoscopic, and macroscopic scales, discussing their strengths and limitations in capturing the intricate processes occurring within these electrochemical devices. Furthermore, we will highlight the recent integration of machine learning techniques into multiscale modeling frameworks, emphasizing their potential to revolutionize the field by accelerating simulations, enabling intelligent design, and uncovering complex relationships.

Despite the promising advancements, challenges remain, such as balancing model complexity and accuracy with computational costs, bridging vast scale gaps, and ensuring robust experimental validation. This review also examines these challenges and outlines future research directions to address them. Ultimately, this review aims to highlight the indispensable role of multiscale modeling in advancing fuel cell and electrolyzer technologies, thereby contributing to the global transition towards a sustainable energy future. The central conclusion emphasizes the transformative potential of multiscale modeling with machine learning to improve the performance, cost-effectiveness, and durability of these critical energy systems.

2. A Taxonomy of Multiscale Simulation Methodologies

Multiscale modeling of electrochemical systems typically involves a hierarchical approach, with distinct computational methods tailored to specific length and time scales. These scales are broadly categorized as microscopic, mesoscopic, and macroscopic as shown in Figure 1. The following Table 1 provides a consolidated overview of these key simulation methods.

Table 1. Overview of key simulation methods in multiscale modeling of electrochemical systems.

Scale	Method	Typical Phenomena Investigated	Key Strengths	Key Limitations/Challenges
Microscopic	Density Functional Theory (DFT)	Bonding, electronic structure, reaction pathways, adsorption energies	High accuracy for ground state properties, fundamental electronic insights	Computationally expensive for large systems, choice of functional, van der Waals interaction, excited states
	Ab Initio Mol. Dynamics (AIMD)	Dynamic processes at interfaces, ion solvation & diffusion, H-bonding	Includes temperature and dynamics from first principles, explicit solvent	Very high computational cost, limited system size and timescale

Table 1. *Cont.*

Scale	Method	Typical Phenomena Investigated	Key Strengths	Key Limitations/Challenges
Mesoscopic	Molecular Dynamics (MD) (Classical)	Ion transport, electrolyte structure, interface dynamics, nanobubble formation	Larger systems and longer times than AIMD, can model complex fluids/materials	Accuracy dependent on force field quality, parameterization can be challenging
	Kinetic Monte Carlo (kMC)	Surface reaction kinetics, diffusion over long times, catalyst aging	Access to experimental timescales, captures stochastic events, spatial inhomogeneity	Accuracy dependent on input rates (from DFT/experiment), lattice representation limitations
	Phase-Field Models (PFM)	Microstructure evolution (e.g., coarsening, phase separation), TPB dynamics	Can model complex morphological changes, no explicit interface tracking	Parameterization can be difficult, computationally intensive for 3D and complex physics
Macroscopic	Continuum Models (PDEs)	Mass, charge, heat transport; current, potential, temp. distributions	Device-level predictions, couples multiple physical phenomena	Simplifies atomic/molecular details, relies on effective parameters, interface models
	Comp. Fluid Dynamics (CFD)	Fluid flow in channels/porous media, thermal management, species distribution	Optimizes flow field design, predicts pressure drop, heat/mass transfer	Turbulence modeling, coupling with electrochemistry, computational cost for complex geometries
	Finite Element Method (FEM) (e.g., COMSOL)	Solves coupled PDEs for multiphysics problems	Versatile for complex geometries & physics, widely available commercial tools	Mesh generation and quality, solver convergence, model setup complexity

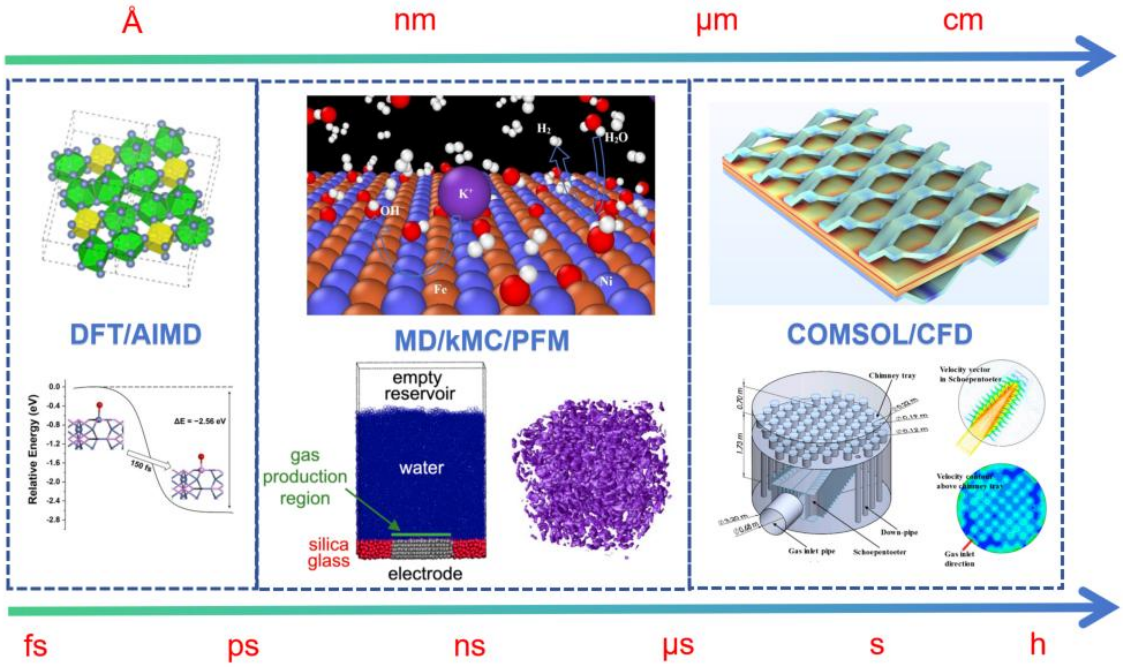

Figure 1. Different-scale simulation methods from microscopic to macroscopic [17–21]. Ref. 17: Copyright 2022, MDPI; Ref. 18: Copyright 2019, ACS; Ref. 19: Copyright 2012, AIP Publishing; Ref. 20: Copyright 2023, https://www.comsol.com/blogs/; Ref. 21: Copyright 2020, MDPI.

2.1. Microscopic Scale

The microscale focuses on the basic electronic and atomic-level processes of electrochemical phenomena. DFT is a key technology in this field, used to study chemical bonding, electronic structure, adsorption and desorption of catalyst surface species, as well as basic reaction steps and energy barriers [22–39]. For instance, DFT can determine the ionization state of the electrocatalyst layer (ECL) and optimize its electronic properties to enhance activity or stability [22].

Ab initio molecular dynamics (AIMD) introduces the motion of atomic nuclei on the basis of DFT, simulating dynamic processes at finite temperatures, such as ion diffusion, interface reconstruction and solvent-molecule interactions. AIMD can accurately simulate charged interfaces, such as the Pt(111)-H_{ad}/water interface, revealing details including the electro-double layer (EDL) structure, adsorbate distribution and water molecule arrangement [25].

Although DFT and AIMD are powerful, the computational cost is high, limiting the system scale and simulation time. This has prompted the development of multi-scale coupling strategies to transfer DFT parameters to low-cost methods and promote the development of machine learning potentials. The accuracy of DFT depends on the selection of exchange-correlation functional, and no single functional performs uniformly well across all chemical systems or for all properties.

There are popular functionals widely employed in chemistry and material simulation, such as PBE, RPBE, and B3LYP. PBE (Perdew–Burke–Ernzerhof) functional is among the most widely used exchange-correlation functionals in electrocatalytic simulations. It effectively captures the electronic delocalization in transition metal (e.g., Pt, Ni) and provides reasonable predictions of adsorption energies for small molecules such as H_2 and O_2, as well as key reaction intermediates like *OH and *OOH on metal surfaces. It is well-suited for high-throughput screening of large-scale systems, including transition metal alloys and oxides. However, PBE suffers from several limitations. For instance, it overestimates the electron delocalization and underestimates van der Waals (vdW) interactions, leading to inaccuracies in simulating the band gap, weakly adsorbed species (e.g., H_2O on carbon supports) and layered materials like MoS_2. It tends to over-bind strongly adsorbed intermediates, which can result in overestimated reaction energy barriers compared to experimental values. Moreover, the spin state is also poorly described. The revised PBE (RPBE) functional addresses part of these issues by modifying the gradient correction term in PBE, thereby mitigating the over-binding of adsorbates and making it more reliable for hydrogen-involving reactions like the hydrogen evolution reaction (HER) and hydrogen oxidation reaction (HOR). Nevertheless, RPBE still lacks an appropriate description of vdW interactions and remains unsuitable for systems dominated by weak intermolecular forces. In addition, B3LYP (Becke, 3-parameter, Lee-Yang-Parr) and HSE (Heyd-Scuseria-Ernzerhof) are frequently used hybrid functionals in modeling, particularly valued for its accuracy in characterizing local electronic structures. It performs well in simulating processes involving bond breaking/formation, such as water dissociation, and in modeling the electronic properties. However, the high computational cost restricts its application to molecular or small periodic systems [24,26,40].

This highlights the challenge of applying DFT to complex electrochemical interfaces, where standard benchmarks may fall short, necessitating trial and error, validation, and sometimes the cherry-pick of functionals tailored to specific environments.

2.2. Mesoscopic Scale

The mesoscopic scale acts as a crucial bridge, linking the atomic-level detail provided by microscopic simulations to the bulk behavior described by macroscopic continuum models. Several computational techniques are employed at this intermediate scale:

Classical and Coarse-Grained Molecular Dynamics (MD): Classical molecular dynamics (CMD) simulations model atomic/molecular interactions using empirical force fields, enabling studies of ion/molecule transport in electrolytes/polymer membranes [41–47], electrode-electrolyte interface dynamics (including solvent arrangements) [48–56], and material degradation mechanisms [57–60]. Coarse-grained MD (CGMD) extends simulations to larger scales by representing atom groups as "beads", successfully applied to phenomena like nanobubble nucleation in water electrolysis [18,60–63]. Though sometimes classified as microscopic (especially when force fields originate from DFT), empirical MD's application to systems with tens of thousands to millions of atoms (nanosecond to microsecond timescales) places it primarily in the mesoscopic domain. The force field parameters, derived from quantum calculations or experimental data, critically determine the simulation's accuracy. Limitations in these parameters can propagate errors to macro-scale conclusions [59].

Kinetic Monte Carlo (kMC): Kinetic Monte Carlo (kMC) is a stochastic method simulating system evolution through discrete-event probabilities (adsorption, diffusion, reactions), with rate coefficients derived from DFT or experiments [64–68]. It excels in studying long-timescale phenomena (ion transport, catalyst evolution) beyond CMD/AIMD limits, enabling applications like CO_2 reduction on copper and SOFC cathode analysis. Unlike static models, kMC captures spatial inhomogeneities and morphology changes, critical for analyzing localized degradation in fuel cells (e.g., nickel coarsening in SOFC anodes) [64].

Phase-Field Models (PFM): PFM is a continuum-based approach that uses a set of continuous field variables (order parameters) to describe the evolution of complex microstructures and morphologies, such as those arising

from phase transformations, grain growth, and particle coarsening in electrode materials [19,69–79]. In SOFCs, for example, PFM can simulate the evolution of the three-phase microstructure (electrode material, electrolyte material, and pore phase), predicting how processes like Ni particle coarsening in anodes affect the distribution of TPBs and, consequently, the electrode's electrochemical performance and long-term degradation [19]. PFM can also be applied to model the evolution of defect structures within materials [69]. The ability of PFM to model such complex microstructural changes is crucial for understanding and mitigating degradation, a major barrier to the commercialization of fuel cell and electrolyzer technologies [80–82].

Mesoscopic models are also employed to simulate transport processes within the complex porous architectures of catalyst layers. These models can describe gas diffusion, liquid water distribution in polymer electrolyte membrane (PEM) systems, and reactant/product transport, thereby revealing how the intricate microstructure of these layers impacts overall device performance.

2.3. Macroscopic Scale

The macroscopic scale addresses the overall behavior of the electrochemical device, integrating information from smaller scales into continuum descriptions that predict system-level performance. Key methods include:

Continuum Models: The modeling of electrochemical devices employs partial differential equation systems (such as the Nernst-Planck equation, Poisson equation, and conservation equation) to simulate the coupled multi-physics transport processes, enabling the prediction of gas distribution, temperature fields, current density, and material concentrations [83–88]. The scale ranges from the nanoscale (porous electrodes) to the macroscopic device level. The improved version of Poisson-Nernst-Planck (PNP) equation, like the Generalized Modified Poisson-Nernst-Planck (GMPNP) formalism, enhances the simulation accuracy in high-concentration electrochemical regions by incorporating the finite ion size effect [86,89–93]. However, the simplification of the continuum model for the double-layer molecular structure and interface dynamics leads to deviations in its prediction results from molecular dynamics simulations. This can lead to inaccurate predictions of local reaction rates and transport behavior, thereby impacting the reliability of device-level performance evaluation. To address this, improved boundary conditions or sub-grid models informed by molecular-level information are needed in continuum simulations [94].

COMSOL Multiphysics and Finite Element Methods (FEM): Commercial software packages like COMSOL Multiphysics are widely used to implement FEM-based macroscopic models for fuel cells and electrolyzers [20,95–98]. These platforms facilitate the coupling of various physical phenomena, including mass transport, fluid flow, ionic and electronic current balance, electrochemical reactions, and heat transfer [20]. Such tools enable engineers to investigate the impact of numerous design parameters and operating conditions on overall cell and stack performance [20,98].

Computational Fluid Dynamics (CFD): CFD specifically focuses on simulating fluid flow, heat transfer, and mass transfer within electrochemical devices, governed by the fundamental conservation equations [99–107]. CFD is crucial for optimizing the design of flow fields in bipolar plates, managing thermal gradients across cells and stacks, ensuring uniform reactant distribution to active sites, and facilitating effective water removal in proton exchange membrane fuel cells (PEMFCs) or product gas removal in electrolyzers [99]. CFD analyses can reveal the effects of electrode porosity, manifold design, gas diffusion layer (GDL) properties, and channel geometry on performance, uniformity, and pressure drop [107]. A common issue highlighted in the application of CFD tools, particularly for SOFCs and SOECs, is the need to fit electrochemical parameters—such as those in the Butler-Volmer equations [106]. This reliance on fitting to experimental data indicates a current gap in achieving truly first-principles-driven multiscale modeling, where parameters would ideally be passed directly from lower-scale simulations.

2.4. Weaving the Scales Together: Coupling Strategies

The essence of multiscale modeling lies in the effective linkage of simulations performed at different scales, allowing information to flow between them to construct a comprehensive picture of the system. Two primary coupling strategies are employed: sequential and concurrent coupling.

Sequential Coupling (Hierarchical or Parameter-Passing): In this approach, information typically flows from smaller, more fundamental scales to larger, more phenomenological scales [21,108–115]. For instance, DFT calculations might be performed to determine reaction energies, activation barriers, or diffusion coefficients. These DFT-derived parameters are then used to parameterize empirical force fields for classical MD simulations or to define the rates of elementary events in kMC simulations. Subsequently, results from these mesoscale simulations, such as effective transport properties (e.g., ionic conductivity, gas diffusivity through a porous layer) or homogenized reaction rates, can be fed as input into macroscopic continuum models that describe the behavior of

the entire cell or stack. First-principles computations are noted for their ability to provide accurate parameters for CMD or mean-field methods, which can then handle much larger and more complex systems [116]. Sequential coupling is generally less computationally demanding than concurrent approaches because the different scale models are run independently or in a one-way sequence. However, this strategy inherently assumes a clear separation of scales and may not adequately capture dynamic feedback mechanisms where processes at a larger scale can influence behavior at a smaller scale in real-time [21].

Concurrent Coupling (Simultaneous or Handshaking): This strategy involves running models for multiple scales simultaneously, with dynamic exchange of information occurring at the interfaces or overlapping domains between these models [110,111,117–122]. Concurrent coupling is more computationally intensive but is essential when there are strong coupling and feedback between phenomena at different scales, and a clear separation is not physically justifiable [21]. The preference for concurrent coupling arises particularly when the information required by one scale model is a complex function of many variables that are actively evolving in another scale model. This is often the case for highly intricate electrochemical interfaces where local atomic configurations, solvent structure, electric fields, and surface charges are strongly interdependent and fluctuate rapidly; under such conditions, sequential coupling might prove insufficient to capture the true system dynamics [119]. A well-established example of concurrent coupling is the Quantum Mechanics/Molecular Mechanics (QM/MM) method [123–132]. In QM/MM, a small, chemically active region of the system (e.g., the site of a catalytic reaction, a bond-breaking event) is treated with a high-accuracy QM method (like DFT), while the larger surrounding environment (e.g., solvent molecules, protein matrix, bulk electrode) is modeled using a computationally less expensive classical force field [127,128]. This hybrid approach aims to balance QM accuracy for the critical reactive part with MM efficiency for the environment, making it suitable for studying enzymatic reactions, reactions in complex solvents, or processes at interfaces [129].

Although Computer-Aided Drug Discovery is a mature field in pharmaceutical research, leveraging computational tools to accelerate drug discovery, its direct translation to "Computer-Aided Materials Discovery" for fuel cells and electrolyzers is more of an aspirational analogy. It signifies the desire for integrated, multi-tool computational workflows for materials design and discovery in electrochemistry. This likely refers to iterative design loops where different simulation tools (potentially spanning multiple scales) inform each other to optimize material compositions, catalyst structures, or electrode architectures for desired electrochemical functionalities. This points towards a future direction of more holistic "Computer-Aided Materials Engineering" platforms [133].

The choice of coupling strategy is a critical decision in any multiscale modeling endeavor, dictated by the specific physics of the problem being addressed, the degree of interaction between phenomena at different scales, and the available computational resources. Table 2 provides a comparison of these coupling strategies.

Table 2. Comparison of coupling strategies in multiscale modeling.

Strategy	Description	Information Transfer Mechanism	Key Examples in Electrochemistry	Advantages	Disadvantages & Computational Considerations
Sequential (Hierarchical)	Models at different scales are run in sequence; output from one scale is input to the next.	Parameter passing (e.g., rate constants, transport coefficients, potentials).	DFT → MD (force field param.), DFT → kMC (rates), Meso → Macro (eff. props.)	Computationally less expensive, conceptually simpler to implement.	Assumes scale separation, no dynamic feedback between scales, error propagation.
Concurrent (Simultaneous)	Models at different scales are run simultaneously, exchanging data dynamically.	Direct data exchange at interfaces/boundaries, shared variables.	QM/MM for catalysis/solvation, adaptive mesh refinement in CFD, coupled particle-continuum methods.	Captures strong coupling and feedback between scales, more physically realistic for some systems.	Computationally very expensive, complex to implement and manage interfaces, numerical stability challenges.

3. Multiscale Modeling in Action: Fuel Cell and Electrolyzer Systems

The theoretical framework of multiscale modeling finds concrete application in addressing specific challenges and advancing the understanding of fuel cell and electrolyzer components and processes. From elucidating fundamental catalyst mechanisms to predicting full-device performance, these methods provide indispensable tools.

3.1. Unveiling Catalyst Mechanisms at the Microscale

The core of efficient fuel cells and electrolyzers lies in catalysts with high activity and stability. First-principles DFT calculations play a crucial role in analyzing the complex mechanisms occurring on the catalyst surface at the atomic and electronic levels. These calculations enable researchers to study the adsorption behavior of reactant molecules (such as H_2, O_2, H_2O, CO_2) and reaction intermediates on various catalyst materials (including traditional platinum group metals and emerging non-precious metal catalysts). DFT can determine the most favorable reaction pathways and calculate the activation energy barriers for each basic step in key electrode reactions (such as ORR and HER in fuel cells, OER and HOR in fuel cells) [17,134–151].

Thousands of related studies have been published. Here, we select two representative works for a brief introduction. As shown in Figure 2a, Zhou et al. focused on the origin of the activity of Fe-N-C catalysts in the ORR [138]. Through DFT combined with experiments, the FeN_4C structure with pyrrole nitrogen (rather than pyridine nitrogen) coordination exhibited the highest ORR activity in acidic media, with its peak potential (0.91 V/RHE) highly consistent with the experimental value (0.89–0.90 V). In alkaline media, the central Fe atom was transformed into O-FeN_4C and OH-FeN_4C active species through axial adsorption of reaction intermediates through the axial adsorption reaction, clarifying the main cause of the high activity of Fe-N-C catalysts under alkaline conditions. This work systematically studied 13 different coordination configurations of Fe-N-C catalysts, combined with the effects of solvation, pH value and potential dynamics, achieving the precise reduction of electrochemical experimental results.

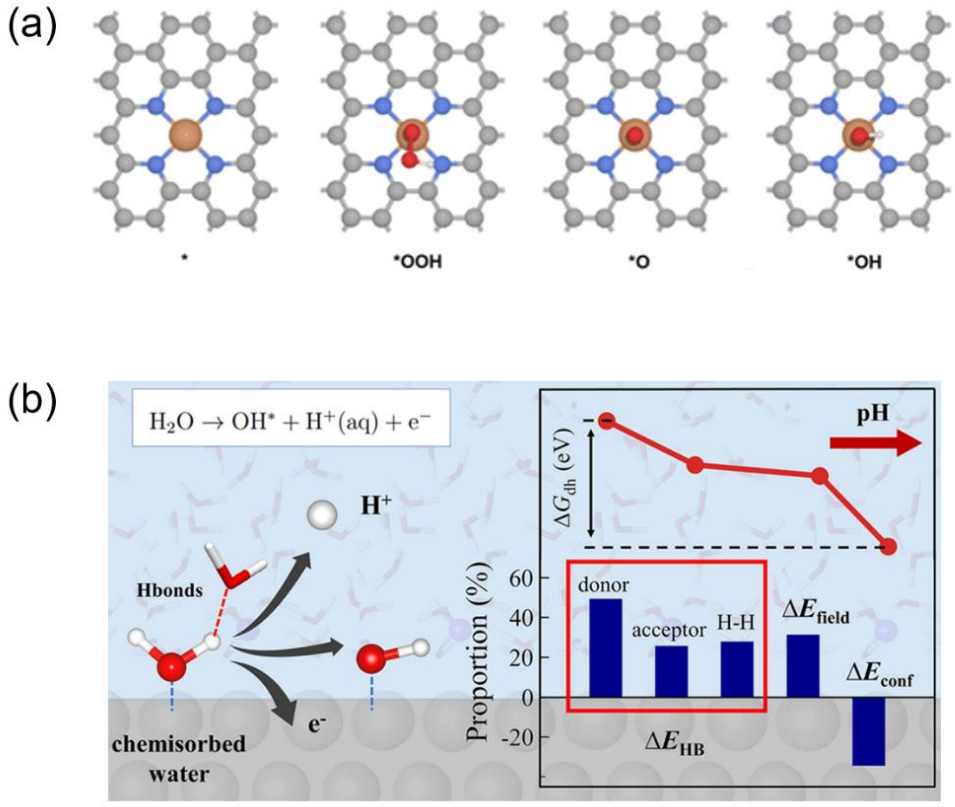

Figure 2. (**a**) Optimized reaction models during ORR catalyzed by pyridinic FeN_4C at zero excess charges, pyridinic FeN_4C slab, *OOH, *O, and *OH. C, gray; N, blue; O, red; H, white; and Fe, brown [138]. Copyright 2022, ACS; (**b**) The dissociation of chemisorbed water is the primary route for OH* adsorption at low pH condition [139]. Copyright 2022, Elsevier.

Le et al. [139] investigated the influence of electrolyte pH on the adsorption/desorption process of OH* on the Pt(111) surface by combining AIMD and free energy perturbation (FEP) methods. It was found that at low pH conditions (pH < 4.3), OH* mainly forms through the dissociation of adsorbed water by chemical adsorption ($H_2O^* \rightarrow OH^* + H^+ + e^-$), and the initial potential shifts negatively with increasing pH, which is consistent with the experimental cyclic voltammogram. At high pH conditions (pH > 5.6), OH^- oxidation ($OH^- \rightarrow OH^* + e^-$) becomes the dominant pathway due to the reduced coverage of chemically adsorbed water (<0.1 ML). The pH

dependence is attributed to the changes in the local hydrogen bond network. At low pH, the virtual H of chemically adsorbed water forms more hydrogen bonds with surrounding water molecules (N_{donor} type), resulting in an increased dissociation energy (0.81 eV, pH = −2.4). At high pH, the hydrogen bond reorganization ($N_{acceptor}/N_{H\text{-}H}$ type) reduces the dissociation energy (0.41 eV, pH = 4.6), while the contributions of interface electric field and conformational changes are relatively small (approximately 0.1 eV in total). This work provides a theoretical basis for optimizing the pH of electrolyte to enhance the reactivity of reactions such as ORR.

3.2. Probing Mesoscale Phenomena: Interfaces, Transport, and Microstructures

Bridging the gap between atomic-level details and macroscopic device behavior, mesoscale simulations investigate phenomena occurring at the scale of nanometers to micrometers over microseconds or longer. These methods are crucial for understanding how interfacial dynamics, ion and molecule transport, and material microstructure evolution influence overall performance and durability.

The water molecule arrangement and charge distribution at the electrode/electrolyte interface can be presented through MD simulation, revealing the interface structural characteristics during the electrocatalytic process [134,152–158]. Molinero et al. focused on the nucleation mechanism and steady-state characteristics of nano-bubbles in electrochemical reactions as shown in Figure 3a [18]. By combining CMD simulation with an electrochemical gas generation algorithm, they simulated the gas generation process on the electrode and successfully reproduced the experimental results of bubble nucleation and stability on platinum nano-electrodes as shown in Figure 3b. The study revealed that surface nano-bubbles must form through heterogeneous nucleation mechanisms and clarified the nucleation conditions on the electrode surface or single-layer micro-plane. Additionally, they also explored how the size and shape of nano-bubbles change with the reaction driving force, and found that although the residual current is independent of the driving force, the size and contact angle of the steady-state nano-bubbles increase with the increase in the driving force. This research provides molecular-level insights into the dynamic behavior of nano-bubbles in electrochemical processes, which is helpful for optimizing electrocatalytic efficiency.

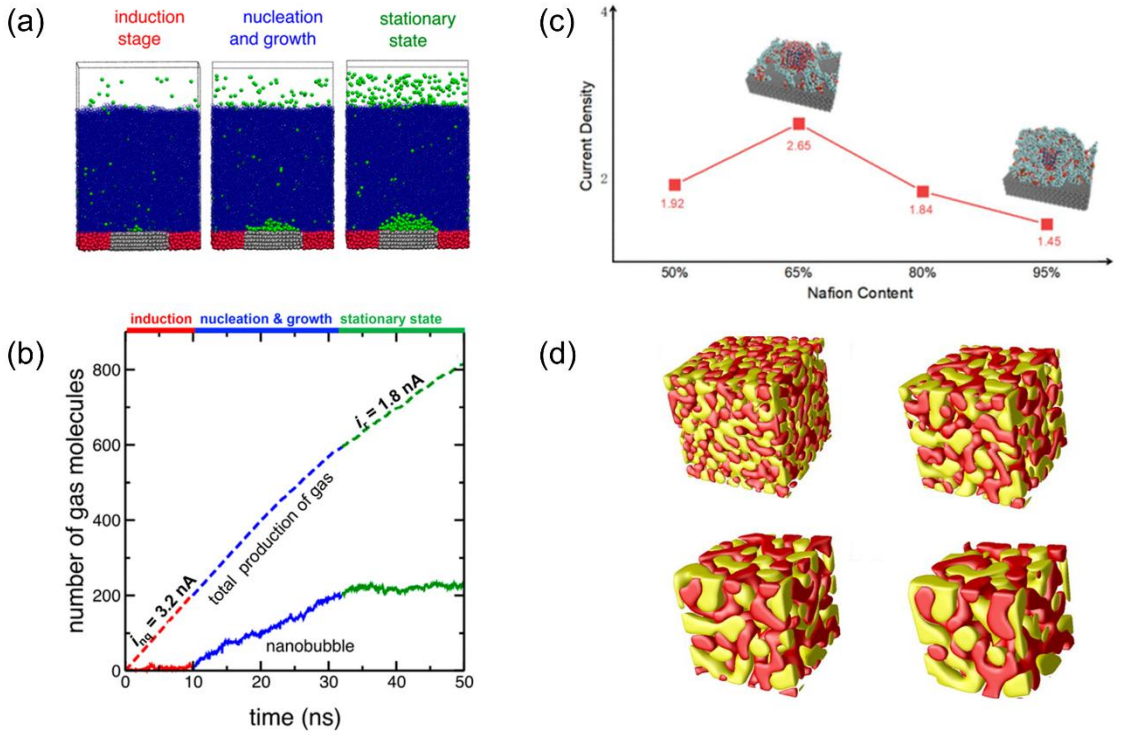

Figure 3. (**a**) Snapshots of the three different stages in the formation of a surface nanobubble [18]. Copyright 2019, ACS; (**b**) Evolution of the number of gas molecules with time. The dashed line represents the total number NG of gas molecules in the simulation cell, while the continuous line shows the number NB of gas molecules in the nanobubble, defined as the largest gas cluster. Red, blue, and green indicate the induction, nucleation and growth, and stationary states, respectively [18]. Copyright 2019, ACS; (**c**) Current density varies with the content of Nafion [159]. Copyright 2024, ACS; (**d**) Temporal microstructural evolution in a three-phase SOFC electrode system. The

electrode-α-phase, electrolyte-β-phase, and pore-γ-phase are represented in red, yellow, and transparent (with volume fraction 30%, 30%, and 40%, respectively) [19]. Copyright 2012, AIP Publishing.

Through coarse-grained MD or kinetic Monte Carlo, the diffusion behavior of ions in the proton exchange membrane can be simulated, and the influence of mass transfer limitations on the performance of fuel cells can be analyzed [159–163]. Zhang et al. combined experimental measurement with MD+MC simulation to reveal the mechanism of the influence of Nafion content on the performance of PEMFCs from the perspective of TPB, providing a molecular-level theoretical basis for optimizing the catalytic layer structure as shown in Figure 3c [159]. This work reported that when the Nafion content was 1.415 mg/m^2, the Nafion coverage on the surface of Pt particles and carbon carriers reached saturation (42.1% and 32.7% respectively), but too low Nafion content led to discontinuous proton conduction paths in the TPB region, resulting in an increase in ohmic loss. While too high Nafion content would block the gas transmission channels. Therefore, to achieve the optimal performance of PEMFCs, the appropriate content of Nafion must be precisely controlled. Wang et al. used two-dimensional infrared spectroscopy and semiclassical simulation to study how water molecules arrange into continuous solvation shells and explained how this structure affects the kinetics of bromide ion transport in polybutadiene-based materials [163]. It was found that water molecules form continuous solvation shells within the membrane. When the reorientation rate of water molecules in the second solvation shell is faster, a stronger hydrogen bond network is constructed, significantly improving the ion transmission efficiency; rapid water molecule rearrangement promotes ion jump transmission, explaining the high conductivity source of halide ions (such as Br^-) in AEM. The dynamic coupling mechanism of ion transmission in polymer electrolytes was revealed, solving the problem of difficult balance between ion conductivity and mechanical strength in traditional materials.

The phase field model (PFM) is used to simulate the evolution of the microstructure of complex materials, such as the porous electrode structures found in SOFC and other electrochemical devices. [19,69–81,164] For instance, Li et al. studied the influence of the three-phase (electrode phase, electrolyte phase, and pore phase) interactions on the performance of SOFC electrodes, proposing a phase field model based on the diffusion interface theory as shown in Figure 3d [19]. They combined the conserved composition order parameter with the non-conserved grain orientation order parameter, simultaneously describing the coupled dynamic process of phase coarsening and grain growth. The simulation results showed that the microscopic morphology of the electrode (such as grain size and pore distribution) significantly depends on the dynamic parameters (such as interfacial energy, diffusion coefficient) and the volume fraction of the three phases. For example, when the electrolyte volume fraction increased from 10% to 30%, the dispersion of the electrode particles decreased, but the length of the TPB increased, optimizing the electrocatalytic activity. In the early evolution stage, the TPB fraction significantly decreased due to phase separation, and the volume fraction balance was required to optimize the performance and stability. This research provides a theoretical tool for the microstructure design and performance optimization of SOFC electrodes, reveals the key mechanism of long-term material degradation, and offers new ideas for the development of efficient and durable electrode [77].

3.3. Predicting Macroscopic Performance and Optimizing Design

Macroscopic models provide the crucial link between fundamental understanding derived from smaller scales and the overall performance and engineering design of full electrochemical cells and stacks [83,84,94,165]. These models typically involve solving systems of coupled partial differential equations (PDEs) that describe transport phenomena and electrochemical reactions at the device level. Take SOFC as an example, the SOFC system consists of components such as the cell, fuel processor, and heat exchanger. Thermodynamic synergy needs to be achieved through a macroscopic model. The macroscopic model can incorporate the research results at the mesoscopic scale (such as the microstructure of the electrode) into the system-level simulation. Parameters calculated by the mesoscopic model, such as pore curvature and the length of the TPB, can be input into the macroscopic model to predict the performance of the cell. This multi-scale coupling solves the problems at the mesoscopic scale, such as the influence of electrode morphology evolution on mass transfer, and provides a theoretical basis for macroscopic design as shown in Figure 4a [165].

Continuum and FEM models are widely used to simulate the distributions of gas flow, temperature, current density, and species concentrations within various components of fuel cells and electrolyzers [83–88,95–98]. These simulations are essential for predicting overall cell voltage, power output, efficiency, and for managing critical operational aspects like water transport in PEM fuel cells or thermal gradients in high-temperature SOFCs. By evaluating system performance under diverse operating conditions (e.g., varying load, temperature, reactant flow rates) and for different geometric designs, these models serve as powerful tools for optimization. Johnson et al. compared the continuum model with MD simulation to reveal the differences in the EDL structure during

electrochemical CO_2 reduction as shown in Figure 4b [86]. They employed the GMPNP equation as the continuum model, which incorporates ion size effects (steric effects) to limit the concentration of cations on the electrode surface and predicts that CO_2 would be excluded from the vicinity of the cathode due to steric hindrance. However, the MD simulation showed that there were two layers of cation adsorption on the Ag electrode surface (with partial dehydration in the inner layer and complete hydration in the outer layer), and the CO_2 concentration at the electrode interface increased due to surface interactions, contrary to the prediction of the continuum model. Additionally, the EDL capacitance calculated by MD (7–9 μF/cm^2) was not affected by electrolyte concentration, cation type, or potential, while the continuum model overestimated the capacitance by ignoring molecular-scale phenomena (such as water molecule polarization oscillations). The study pointed out that the continuum model is effective at the macroscopic scale but needs to incorporate atomic-level details for improvement, such as considering EDL or dilute solution theory. It established a theoretical foundation for refining multiscale models through direct comparisons, enabling more accurate simulations of electrochemical CO_2 reduction systems [86].

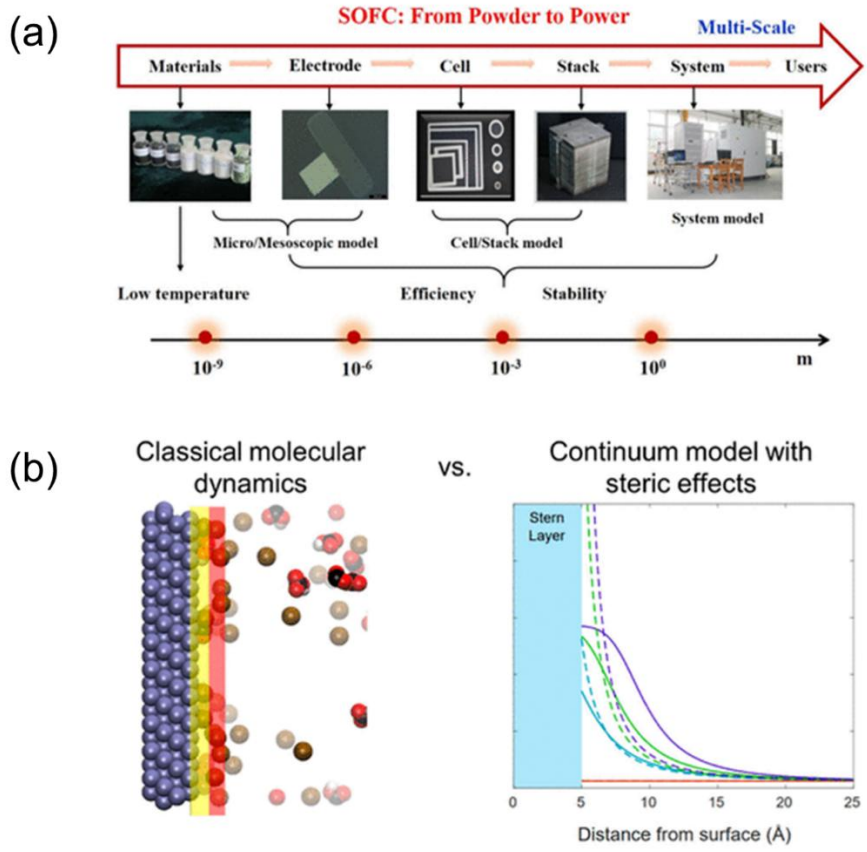

Figure 4. (**a**) Relationship between research objects, research scale, and modeling methods for SOFCs [165]. Copyright 2025, ACS; (**b**) Comparison of EDL calculated by CMD and Continuum model with steric effects [86]. Copyright 2024, ACS.

CFD serves as the core tool for macroscopic modeling, playing a crucial role in the design of fuel cell flow fields, thermal management, and optimization of reactant distribution [99–108]. By quantifying the coupling effects of configurations such as serpentine and parallel flow channels with electrode porosity and gas diffusion layer characteristics, CFD can accurately predict the influence of key parameters such as pressure drop and flow uniformity on cell performance. This macroscopic modeling approach can reveal complex phenomena that are difficult to capture through traditional experiments, such as local "hot spots" caused by uneven flow fields or regions with insufficient reactants [95]. These hidden defects can lead to accelerated material degradation and significantly shorten the cell lifespan. Commercial software such as COMSOL Multiphysics provides an integrated platform for such multi-physics simulations, enabling engineers to systematically study the interaction between design parameters such as flow channel size and electrode conductivity and operating conditions such as gas composition and flow rate, thereby optimizing the overall performance of the battery stack [98]. However, it is important to note that the reliability of the macroscopic model highly depends on the accuracy of the underlying

sub-models, including parameters such as Butler-Wolfe equations in electrochemical kinetics and effective diffusion coefficients in porous medium transport processes. If these fundamental parameters are derived from inaccurate low-scale simulations or extrapolations from limited experimental data, it will lead to macroscopic prediction deviations, not only affecting the optimization effect of the design, but also potentially causing the actual device performance to be far below expectations [97,98]. Therefore, establishing a cross-scale verification mechanism to ensure the accuracy of parameter transfer from microscopic properties to macroscopic behavior is the key to improving the practicality of CFD modeling.

The performance of electrochemical devices is highly dependent on the distribution and transport of ions within complex pore structures, as well as the EDL formation. However, traditional experimental and simulation methods face significant challenges in capturing the multiscale phenomena spanning from nanoscale EDL formation to macroscopic device performance. There exists a substantial gap, up to five orders of magnitude, between the time scales of ion distribution equilibrium at porous electrode surfaces observed experimentally and those predicted by micro-/mesoscale simulations. Recently, Lian et al. developed a physics-based modelling approach, proposing a "stack-electrode model" in which porous electrodes are represented as a series of parallel, permeable electrode sheets with spacing simulating the pore size [166]. This model employs the PNP equations to describe ion transport and shows strong agreement with equivalent circuit models at low applied potentials, reflecting the slow charging behavior resulting from the high surface area of porous electrodes. At high potentials, the charging dynamics exhibit two-time scales: an initial charge relaxation and a slower process controlled by ion diffusion. Notably, when the pore size is comparable to the Debye length, these two-time scales converge, consistent with the observed behavior of porous electrodes. Validated using experimental parameters (such as carbon electrode thickness, pore size, and electrolyte concentration), the model predicts electrochemical time scales within the same order of magnitude as experimental values, successfully bridging the gap between theory and experiment. Further application of the stack-electrode model to cyclic voltammetry (CV) simulations established a quantitative relationship between CV response and microstructural parameters [167]. At high potentials, CV curves exhibit strong scan rate dependence. Pore size distribution significantly influences the CV response. Non-uniform distribution leads to deviations in estimated effective pore size and relaxation time, underscoring the necessity of accounting for the complex structure of real porous electrodes in the model. With few fitting parameters, the model can reproduce experimental CV curves across a wide range of scan rates, providing a novel approach for the quantitative characterization of porous electrodes.

3.4. Analysis of Multiscale Modeling Needs for Other Typical Electrochemical Devices

In addition to the SOFC and PEMFC systems, which have been extensively discussed as representative systems, solid oxide electrolysis cells (SOEC), anion exchange membrane electrolyzers (AEM electrolyzers), and reversible fuel cells (RFC) are also important electrochemical devices. However, their working principles differ significantly. Understanding these differences is critical for ensuring the reliability of model construction. Below is a concise comparison of the core multiscale modeling requirements for these systems.

Solid-Oxide Electrolysis Cells (SOEC): As the reverse process of SOFC, SOEC operates under high-temperature electrolysis conditions (600–800 °C) to produce hydrogen/oxygen. Its multiscale modeling needs focus on oxygen ion transport and electrode degradation in reducing atmospheres [19,86]. At the microscopic scale, DFT/AIMD is required to calculate the activation energy barriers for the OER path on cathodes and oxygen vacancy diffusion in electrolytes, which differs from SOFC's emphasis on the ORR path. At the mesoscopic scale, phase-field models (PFM) are more critical for simulating anode particle coarsening under reducing conditions (an issue more pronounced in SOEC than in SOFC) and its impact on triple-phase boundary (TPB) length [77]. At the macroscopic scale, CFD models need to couple thermal gradients with electrolysis kinetics (e.g., Butler-Volmer parameters for OER), rather than focusing on fuel oxidation as in SOFC.

AEM Electrolyzers: These low-temperature devices (25–80 °C) rely on OH- conduction in anion-exchange membranes, with their multiscale modeling requires primarily centered on anion transport efficiency and membrane stability [41,163]. At the microscopic scale, DFT simulations prioritize studying OH^- adsorption/desorption processes on non-precious metal catalysts (e.g., M-N-C) and the influence of cations (e.g., K^+) on water structure, which differs from PEMFC's focus on H^+ transport. At the mesoscopic scale, CMD and CGMD are crucial for simulating OH^- migration in AEMs (e.g., polybenzimidazole-based membranes) and the dynamic formation of water channels, which directly determines ionic conductivity. At the macroscopic scale, CFD models need to optimize alkaline electrolyte flow (to mitigate AEM swelling) and avoid local pH gradients. These challenges are less prominent in PEMFC.

Reversible Fuel Cells (RFC): RFCs switch between fuel cell (power generation) and electrolysis (hydrogen production) modes, requiring multiscale models to handle dynamic cross-mode coupling [165]. At the microscopic

scale, DFT must simultaneously predict the energy barriers for ORR (fuel cell mode) and OER (electrolysis mode) on bifunctional catalysts (e.g., Pt-Ir alloys), a dual requirement not needed for single-mode devices. At the mesoscopic scale, kMC simulations need to capture the reconstruction of catalyst active sites during mode switching (e.g., oxide formation/dissolution on Ir surfaces). At the macroscopic scale, FEM models must couple transient mass/charge transport with dynamic electrochemical reactions. For example, by adjusting flow field parameters to avoid water flooding in fuel cell mode and electrolyte depletion in electrolysis mode.

3.5. Synergistic Multiscale Integration

The core of multi-scale modeling lies in the collaborative integration of cross-scale simulations [168–172]. Through the information exchange and verification among models at different levels, a comprehensive understanding of the device behavior from fundamental principles to macroscopic performance can be achieved. A typical approach is to use the results of high-precision microscopic simulations (such as DFT calculations for catalytic activity parameters) as inputs for mesoscopic and macroscopic models [170,172–177]. For example, mesoscopic transport simulations can output effective reaction rates or transport coefficients, which can then be further used to predict the overall performance of fuel cells/electrolyzers. The analysis of atomic-level interface reaction mechanisms (such as charge transfer steps) provides physically clear parameters for macroscopic continuum models (such as the Butler-Volmer equation). Typical cases include the coupling study of micro-mechanics simulation with two-dimensional continuum models for electrochemical CO_2 reduction, or the combination of macroscopic device models with mesoscopic seepage theory for analyzing the electrode connectivity of SOEC [168]. However, there are challenges in cross-scale information transmission: the assumptions of upscaling (such as averaging of atomic properties) and downscaling (such as defining the microenvironment based on macroscopic conditions) need to be rigorously verified; otherwise, errors may be introduced [174]. Moreover, successful integration requires iterative feedback. The abnormal phenomena discovered by the macroscopic model (such as hotspots in current density) may drive the optimization of the low-scale simulation, thereby revealing the local mechanisms (such as changes in material properties). This iterative cycle of cross-scale mutual confirmation is a key strategy for constructing complex electrochemical systems and achieving accurate and comprehensive understanding. Table 3 provides illustrative examples of how multiscale modeling is applied to various components and processes within fuel cells and electrolyzers [168–177].

Table 3. Illustrative applications of multiscale modeling in fuel cell and electrolyzer components [168–177].

Component/Process	Dominant Scale(s) Modeled	Key Simulation Techniques Employed	Major Insights/Outputs
Catalyst Layer ORR/OER/HOR/HER Mechanism	Microscopic (DFT, AIMD), Mesoscopic (kMC)	DFT, AIMD, kMC, Microkinetic Modeling	Reaction pathways, activation energies, turnover frequencies, catalyst descriptors, surface coverage
Ion Transport in PEM/AEM/Solid Electrolytes	Microscopic (AIMD), Mesoscopic (MD, CGMD, kMC)	AIMD, CMD, kMC, Nernst-Planck (continuum linking)	Diffusion coefficients, conductivity, transport mechanisms, effect of hydration/morphology
SOFC Anode/Cathode Microstructure Degradation	Mesoscopic (PFM, kMC), Macro (Coupled CFD)	PFM, kMC, FEM	Particle coarsening, TPB length evolution, porosity changes, impact on effective properties, lifetime prediction
PEMFC Water Management	Mesoscopic (Pore-Network Models, LBM), Macro (CFD, COMSOL)	Pore-scale modeling, CFD, Multiphase flow models	Water distribution, flooding/drying phenomena, impact of GDL/channel design on water removal
Full Cell/Stack Thermal & Flow Distribution	Macroscopic (CFD, FEM/COMSOL)	CFD, Heat transfer models, FEM, Electrochemistry Module of ANSYS Fluent, multiphase flow module of STAR-CCM+	Temperature profiles, current density distribution, flow uniformity, pressure drop, hotspot identification
Electrolyzer Nanobubble Formation & Dynamics	Mesoscopic (CGMD, CMD)	MD, Multiphase MD	Nucleation sites, growth rates, bubble detachment, impact on electrode coverage and overpotential
Solid Electrolyte Interphase (SEI) Evolution	Microscopic (AIMD), Mesoscopic (kMC, MD)	AIMD, kMC, MD	SEI composition, morphology, growth mechanisms, impact on ion transport and stability

4. The Ascent of Machine Learning in Multiscale Electrochemical Modeling

Machine learning (ML) is the core branch of artificial intelligence, enabling computers to autonomously discover patterns from data and perform tasks such as prediction, classification, or decision-making through algorithms. Its essence is to construct mathematical models and use statistical methods to optimize parameters, thereby simulating the human learning process. In recent years, with the rapid development of ML technology, it has demonstrated unique advantages in solving multiscale simulation problems, providing new possibilities for the design, optimization, and control of fuel cells and electrolyzers. In the multiscale simulation of fuel cells and electrolyzers, ML technology has been widely applied in various aspects, including electrocatalyst design, membrane electrode assembly optimization, flow-field management, and performance prediction. By integrating the physical mechanisms at the microscale with the system behavior at the macroscale, ML methods can significantly improve simulation efficiency and enhance prediction accuracy, thus promoting the research and development process of new energy conversion devices [178–192]. Here we will delve into the four core roles of ML in the simulation of fuel cell and electrolyzer systems: accelerating material design and screening, reaction mechanism analysis, cross-scale parameter transfer and macroscopic model calibration, complex model modeling and properties prediction.

4.1. Acceleration of Material Design and Screening

The core performance of fuel cells and electrolytic cells (such as catalytic activity, stability, and mass transfer efficiency) is fundamentally determined by material properties (such as the active site structure of the catalyst, the ionic conductivity of the electrolyte, and the pore structure of the electrode). ML through high-throughput computing or data mining of experimental results, quickly screens out potential high-performance materials (such as electrocatalysts and PEM), providing a specific research platform for subsequent reaction mechanism analysis, parameter transfer, and model construction.

For example, Liang et al. focused on the design challenge of low-platinum catalysts for PEMFCs. ML models were used to statistically quantify the vast configuration space and evaluate the impact of chemical ordering on thermodynamic stability [185]. Through screening, it was discovered that the introduction of Cu/Ni elements could induce Co-Cu/Ni disorder, providing additional stability energy, thereby promoting the ordering process and achieving a balance between particle size and order degree. Based on the theoretical predictions, the research team successfully prepared small-sized and highly ordered ternary Pt_2CoCu and Pt_2CoNi catalysts. These catalysts exhibit excellent electrochemical performance, including a large electrochemical active surface area of approximately 90 m^2/g_{Pt} and a high specific activity of approximately 3.5 mA/cm^2, with a mass activity exceeding the target set by the US Department of Energy. Shang et al. constructed a universal ML framework that can minimize manual intervention and prior physical knowledge to screen out single-doped, double-doped, and triple-doped RuO_2 catalysts, as shown in the Figure 5a [182]. Within this framework, a geometric feature-based clustering extension (CE) model was employed to assess the stability of RuO_2-based catalysts as shown in Figure 5a, while convolutional neural networks (CNNs) leveraging projected density of states (DOS) signatures from active sites, rather than relying solely on energy band centers or atomic descriptors, achieved superior predictive accuracy for OER activity in Figure 5b. Both models demonstrated exceptional predictive performance for doped RuO_2 systems, achieving remarkable R^2 coefficients (>0.90 for CE and >0.95 for CNN) when correlating predictions with DFT calculations, significantly surpassing the accuracy of earlier approaches. Through exploration of the chemical space for 3d transition metal-substituted RuO_2 systems, the researchers identified three high-performance OER catalysts: $Ru_{41}Zn_7O_{96}$, $Ru_{41}Fe_3Zn_4O_{96}$, and $Ru_{39}Co_1Cu_4Zn_4O_{96}$. This work not only establishes a dedicated ML framework for RuO_2-based catalyst prediction but also introduces a generalized paradigm for accelerated catalytic material discovery, integrating geometric and electronic structure descriptors to bridge atomic-scale insights with macroscopic performance optimization.

4.2. Analysis of the Reaction Mechanism

The reaction mechanism analysis is based on material design, delving into the microscopic scale (atomic/molecular level) to reveal the root causes of material properties, and at the same time providing a "microscopic parameter source" for the transfer of cross-scale parameters. Its core lies in using algorithms to uncover the deep laws of the reaction system and achieving precise mapping from microscopic mechanisms to macroscopic properties [193–203]. For example, the adsorption energy of key reaction intermediates on the electrode surface determines the reaction pathway. ML methods can be used to quickly predict the adsorption energy of key species based on surface structure and electronic features.

Fung et al. proposed a ML model based on convolutional neural networks (CNN), so-called DOSnet as shown in Figure 6. This model automatically extracts key features from the electronic density of states (DOS) to achieve high-precision prediction of adsorption energy, thereby facilitating in-depth exploration of reaction mechanisms [199]. The DOSnet model was applied to various adsorbates and surfaces, and the average absolute error of the predicted adsorption energy reached the order of 0.1 eV, which is sufficient to replace DFT calculations and significantly accelerates the simulation and prediction of the adsorption process. More importantly, this model can predict the external perturbation of the electronic structure without additional DFT calculations, which provides the possibility of accelerating the discovery of materials and catalysts by exploring the electronic space. The projected DOS was used as the input, avoiding the cumbersome process of manually designing descriptors in traditional methods. This data-driven approach not only improves the prediction efficiency but also enhances the interpretability of the model, enabling researchers to better understand the electronic structure changes in the adsorption process and thereby reveal the reaction mechanism.

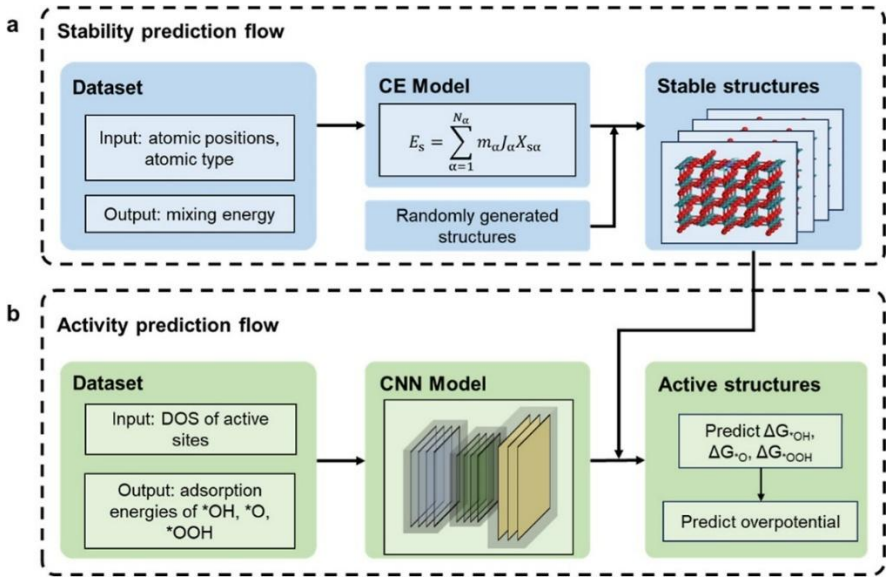

Figure 5. High-throughput screening flows of (**a**) catalytic stability based on the cluster expansion (CE) model and (**b**) catalytic activity based on the convolutional neural network (CNN) model. During the screening operation, the stability of plenty of randomly generated doping structures was first evaluated by the CE model to obtain highly stable structures, whose activities were then estimated by the CNN models to further screen out highly active structures [182]. Copyright 2025, ACS.

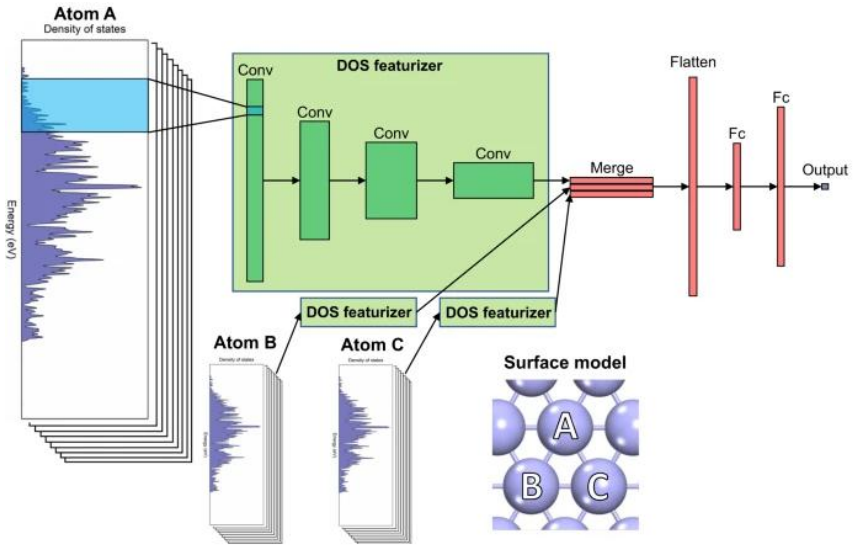

Figure 6. General schematic of the DOSnet model. The site-projected DOS of a surface atom serves as the input (light blue) which goes through a series of convolutional layers (green), followed by fully connected layers (red) and a final output layer. For additional atoms, the same convolutional layers are used with shared weights before being merged with the fully connected layers [199]. Copyright 2021, Springer.

4.3. Cross-scale Parameter Transfer and Macroscopic Model Calibration

The cross-scale parameter transfer and the results of reaction mechanism analysis are used to address the "scale gap" problem in multiscale simulations and provide a "data interface" for macro model calibration and complex model construction. Traditional methods focus on parameter transfer between models and boundary condition matching, while ML technology significantly improves the efficiency and accuracy of cross-scale simulations through feature extraction, proxy model construction, and active learning. The multiscale simulation of fuel cell/electrolyzers involves a scale transition from microscopic (atomic reactions) → mesoscopic (electrode pore structure) → macroscopic (battery system). Parameters at different scales (such as microscopic reaction rates, mesoscopic mass transfer coefficients, and macroscopic voltage current) cannot be directly reused. ML model achieves the transfer of microscopic parameters to the macro model by constructing parameter mapping relationships (such as converting the activation energy calculated by DFT into parameters of the macro reaction kinetics equation); at the same time, it calibrates the transferred parameters using macroscopic experimental data (such as polarization curves) to ensure the consistency of models at different scales [180,185,204–207].

Armstrong et al. utilized the deep learning algorithm DualEDSR in conjunction with X-ray micro-computed tomography technology to construct a high-precision three-dimensional model with a resolution of 700 nm and an area of 16 mm^2 [204]. This breakthrough overcomes the trade-off between resolution and field of view in proton exchange membrane fuel cell modeling, enabling the transfer of cross-scale parameters from nano-scale electrocatalysts to millimeter-scale flow fields. The DualEDSR algorithm expands the field of view by approximately 100 times through training with low-resolution global images and local high-resolution images, generating an ultra-resolution model beyond the hardware limit and achieving cross-scale connection from nano-scale electrocatalysts to millimeter-scale flow fields. At the same time, the convolutional neural network is used to precisely segment the internal structure of the battery (such as the gas diffusion layer and microporous layer), extract key features of multi-scale water aggregation and transport, and provide a structured data basis for parameter transfer. Finally, based on the generated high-resolution model, large-scale multiphase flow simulations are directly conducted to reveal the water management mechanism in dry and submerged areas, quantify the impact of microscopic structure changes on macroscopic performance, and achieve a "modeling-verification-optimization" closed loop. This research builds a bridge for cross-scale parameter transfer through ML, integrating local high-resolution details with global low-resolution data, significantly improving modeling accuracy and efficiency.

4.4. Modeling Complex Interfaces and Predicting Properties

Complex model construction is a systematic integration of material design, mechanism analysis, and cross-scale transfer results, ultimately serving the prediction and optimization of device performance. The operation of fuel cells and electrolytic cells involves electrochemical reactions, multi-component mass transfer, heat conduction, and other multi-physical field couplings. ML integrates material property data, microscopic mechanism parameters, and the coupling relationships of cross-scale transfer to construct complex models (such as full battery performance prediction models, degradation lifetime models). At the same time, the output of the complex model can in turn guide material design and screening, verify the correctness of reaction mechanism analysis, and thus form an iterative closed loop of "material design → mechanism analysis → parameter transfer → model construction → feedback optimization". Beyond accelerating existing simulation workflows or enabling new design paradigms, ML algorithms excel at analyzing large, complex datasets—whether from experiments or simulations—to uncover hidden correlations, identify key descriptive features, and build predictive models for properties and phenomena that are challenging to capture with traditional physics-based models alone [208–216]. This is particularly relevant for understanding the intricacies of electrochemical interfaces.

As a typical example, a deep neural network enhanced mesoscopic thermodynamic (DeepMT) model has been proposed by Lian et al., to provide foundational understanding of the electrochemical properties of the electrode/electrolyte interface [214]. This model deeply integrates the deep operator network (DeepONet) with the mesoscopic thermodynamic model based on classical DFT, constructing a complex model that can handle both microscopic ion interactions (such as hard sphere repulsion, Coulomb force) and macroscopic external field effects (such as electric field, concentration). By replacing the complex functional solution process in traditional numerical methods with neural networks, this model achieves efficient integration and calculation of cross-scale information, preserving the rigor of the physical model while significantly improving the simulation efficiency of complex interface systems. The DeepMT model learns from the training data of DFT and directly predicts the ion density distribution at the electrode/electrolyte interface. It not only captures the oscillatory distribution of ions and charge reversal phenomena but also further deduces key interface properties such as adsorption capacity, surface charge, and differential capacitance. After being verified by 5 cases, this method is effective under different boundary

conditions, multi-phase and multi-physical field scenarios. The calculation time is reduced by 50 to 1000 times compared to the finite element method, providing a reliable alternative solution for parameterized reaction transport equations in porous media, and facilitating the study of complex phenomena [215].

The machine chemist system developed by the University of Science and Technology of China has achieved a revolutionary autonomous synthesis of oxygen-producing catalysts for Martian meteorites through the deep integration of machine learning and multi-scale simulation [216]. This system first uses laser-induced breakdown spectroscopy to conduct atomic-scale characterization of the meteorite composition, and combines quantum chemical calculations to build a theoretical database; then, through molecular dynamics simulation, it predicts the behavior of material interfaces and establishes a cross-scale correlation model between microstructure and macroscopic properties. The machine learning algorithm plays a core role in this process: It uses graph neural networks to process non-equilibrium material data, solving the accuracy bottleneck of traditional DFT calculations in high-entropy alloy systems; It develops a transfer learning framework to transfer knowledge from the Earth's catalyst database to the Martian meteorite system, significantly improving the efficiency of small-sample learning; It builds a "computational-experimental" loop through Bayesian optimization, achieving the locking of the optimal solution within 6 weeks from 376,000 formula combinations, which is 10^5 times faster than traditional methods. Experimental verification shows that the AI-designed catalyst can operate stably for 550,000 s at a current density of 10 mA/cm^2, with an oxygen evolution overpotential as low as 445.1 mV. Its performance advantage directly stems from the collaborative optimization of multi-scale parameters such as electron transfer potential barriers and active site distribution by machine learning. This achievement not only provides a paradigm for in-situ utilization of extraterrestrial resources but also pioneers a new model of "AI + multiscale simulation" for material development—by integrating real-time data from quantum-scale calculations, mesoscopic-scale simulations, and macroscopic performance tests, it breaks through the scale barriers in traditional research and establishes a general methodology for extreme environment material design [217–220].

5. Challenges and Future Outlook

Currently, multi-scale modeling of fuel cells and electrolyzers faces three major challenges.

(1) The trade-off between accuracy and efficiency is evident: quantum mechanics methods (e.g., DFT) can capture atomic-level interactions but are computationally demanding, while macroscopic continuum models are efficient at the device scale but often neglect the microscopic mechanisms [161].
(2) The discontinuity of scale coupling is particularly prominent, extending from femtosecond-level charge transfer processes to material degradation over years—spanning six orders of magnitude in time—and from nanoscale catalytic layers to micrometer-scale systems.
(3) Existing models struggle to achieve dynamic correlation across all scales. The electrochemical active interface, as the core of energy conversion, requires more accurate parameterization for its dynamic reconstruction, multiphase contact, and defect evolution, yet limited experimental verification often causes model predictions to diverge from real operating conditions.

Furthermore, advances in multi-physics coupling algorithms remain limited, and persistent hardware constraints on computational resources continue to hinder the adoption of high-precision simulations in industrial design [105]. Addressing computational cost barriers is essential for promoting the practical application of multi-scale modeling. Two strategies have demonstrated significant promise. First, GPU acceleration has brought transformative improvements to large-scale simulations. For example, GPU-optimized DFT code, such as VASP-GPU, can reduce the computation time for simulating ORR mechanisms on Pt alloy catalysts by 5–10 times. Meanwhile, GPU-parallelized molecular dynamics codes (e.g., LAMMPS-GPU) allow microsecond-scale simulations of electrolyte ion transport in PEMs containing millions of atoms, dramatically improving the efficiency of cross-scale parameter transfer (e.g., from DFT to MD). Second, reduced-order models (ROMs) provide a complementary approach. By simplifying high-fidelity models, for instance, replacing full PDE solvers with machine learning surrogates or reduced-basis methods, ROMs preserve essential physical insights while reducing computational expense by one to two orders of magnitude. As an example, ROMs derived from macroscopic CFD models of SOFCs can rapidly predict stack-level temperature distributions with errors below 5% compared to full simulations, thereby enabling real-time optimization of operating conditions. When integrated within multi-scale coupling frameworks, these strategies can mitigate hardware limitations and help bridge the gap between high-precision modeling and industrial design requirements [105].

The future breakthroughs in multi-scale modeling are expected to depend on four major technological pillars:

(1) By developing a unified framework to simultaneously couple electrochemistry, fluid heat transfer, mechanical stress and chemical reactions, multiple physical fields can be deeply integrated. It is expected to achieve full-scale simulation from molecular reactions to system outputs
(2) The growing use of AI is expected to transform modeling approach, from using ML to accelerate DFT calculations, to the development of data-drive surrogate models that replace traditional partial differential equation solvers, and to the discovery of new catalytic materials using generative AI [206,207].
(3) The collaborative innovation of experiments and computations through the closed-loop interaction of high-throughput experimental platforms and modeling tools can quickly validate model assumptions and feedback parameter optimization, forming a forward iteration of materials-models-equipment.
(4) The development of a standardized ecosystem involves creating modular modeling platforms, establishing cross-scale parameter libraries, and defining data-sharing protocols. Together, these efforts can help move the field to shift from fragmented research towards more collaborative innovation.

The advancement of digital twin technology will enable closer integration of real-time simulation with physical systems, supporting full life-cycle management of fuel cell technologies—from design optimization to operation prediction—and providing a foundation for the hydrogen economy.

6. Conclusions

Multiscale modeling has become an important tool for studying, designing, and improving fuel cells and electrolyzers. By bridging processes across different length and time scales inherent, from electron transfer at the quantum level to performance at the device scale, these simulations provide insights that are difficult to obtain from experiments or single-scale modelling alone. This review has summarized the methods employed at the microscopic, mesoscopic, and macroscopic scales, the strategies for coupling these models, and their applications in studying reaction mechanisms, describing transport processes, predicting microstructural changes, and improving device design and operation. The integration of ML techniques is increasing reshaping the field. ML-derived potentials can significantly accelerate computationally intensive atomistic simulations, while data-driven approaches help identify novel material descriptors and allow efficient exploration of vast design spaces. Combining physics-based modeling and data offers opportunities to accelerate materials discovery, optimize electrode and cell architectures, and improve the predictive accuracy of models for long-term performance and degradation. The development of multiscale modeling in electrochemistry shows similarities to its use in other complex material systems, such as biomaterials. This makes it possible to benefit from cross-disciplinary progress in algorithms, coupling techniques, and validation methods.

Despite notable progress, challenges remain, including high computational cost, difficulties in bridging large scale gaps, accurate description of dynamic interfaces, robust parameterization, and the need for thorough experimental validation. Future directions are expected to involve enhanced multiphysics coupling, broader integration of AI/ML methods, closer synergy with high-throughput experiments, and the establishment of standardized open platforms and digital twins. The effectiveness of multiscale modeling will ultimately accessed by its ability to improve the cost, performance, and durability of real-world fuel cell and electrolyzer devices. By advancing the scientific understanding and providing predictive tools to address current limitations, multiscale simulation can support the wider deployment of clean energy technologies and contribute to global climate and energy goals.

Author Contributions

The manuscript was written through contributions of all authors. All authors have read and agreed to the published version of the manuscript.

Funding

This work was supported by the National Key Research and Development Project of China (2023YFB4005900) and the National Science Foundation of China (No. 52171022). It is sponsored by the State Key Laboratory of Intelligent Green Vehicle and Mobility under Project No.KFZ2403.

Conflicts of Interest

The authors declare no conflict of interest.

Use of AI and AI-assisted Technologies

No AI tools were utilized for this paper.

References

1. Lebrouhi, B.E.; Djoupo, J.J.; Lamrani, B.; et al. Global hydrogen development—A technological and geopolitical overview. *Int. J. Hydrogen Energy* **2022**, *11*, 7016–7048.
2. Ferriday, T.B.; Middleton, P.H. Alkaline fuel cell technology—A review. *Int. J. Hydrogen Energy* **2021**, *46*, 18489–18510.
3. Yang, Y.; Li, P.; Zheng, X.; et al. Anion-exchange membrane water electrolyzers and fuel cells. *Chem. Soc. Rev.* **2022**, *51*, 9620–9693.
4. Firouzjaie, H.A.; Mustain, W.E. Catalytic Advantages, Challenges, and Priorities in Alkaline Membrane Fuel Cells. *ACS Catal.* **2020**, *10*, 225–234.
5. Zhao, G.; Rui, K.; Dou, S.; et al. Heterostructures for Electrochemical Hydrogen Evolution Reaction: A Review. *Adv. Funct. Mater.* **2018**, *28*, 1803291.
6. Zou, X.; Zhang, Y. Noble metal-free hydrogen evolution catalysts for water splitting. *Chem. Soc. Rev.* **2015**, *44*, 5148–5180.
7. Zhang, X.; Chan, S.H.; Ho, H.K.; et al. Towards a smart energy network: The roles of fuel/electrolysis cells and technological perspectives. *Int. J. Hydrogen Energy* **2015**, *40*, 6866–6919.
8. Hauch, A.; Kungas, R.; Blennow, P.; et al. Recent advances in solid oxide cell technology for electrolysis. *Science* **2020**, *370*, eaba6118.
9. Zhou, Y.; Zhong, H.; Chen, S.; et al. Proton exchange membrane-based electrocatalytic systems for hydrogen production. *Carbon Enery* **2024**, *7*, e629.
10. Andreaus, B.; Eikerling, M. Active site model for CO adlayer electrooxidation on nanoparticle catalysts. *J. Electroanal. Chem.* **2007**, *607*, 121–132.
11. Braatz, R.D.; Alkire, R.C.; Seebauer, E.; et al. Perspectives on the design and control of multiscale systems. *J. Process Contr.* **2006**, *16*, 193–204.
12. Blanquer, G.; Yin, Y.; Quiroga, M.A.; et al. Modeling Investigation of the Local Electrochemistry in Lithium-O_2 Batteries: A Kinetic Monte Carlo Approach. *J. Electrochem. Soc.* **2015**, *163*, A329–A337.
13. Shin, H.; Yoo, J.M.; Sung, Y.-E.; et al. Dynamic Electrochemical Interfaces for Energy Conversion and Storage. *JACS Au* **2022**, *2*, 2222–2234.
14. Magnussen, O.M.; Groß, A. Toward an Atomic-Scale Understanding of Electrochemical Interface Structure and Dynamics. *J. Am. Chem. Soc.* **2019**, *141*, 4777–4790.
15. Cheng, J.; Liu, X.; VandeVindele, J.; et al. Redox Potentials and Acidity Constants from Density Functional Theory Based Molecular Dynamics. *Acc. Chem. Res.* **2014**, *47*, 3522–3529.
16. Wang, J.; He, H.; Wu, Y.; et al. Review on Electric Resistance in Proton Exchange Membrane Fuel Cells: Advances and Outlook. *Energy Fuels* **2024**, *38*, 2759–2776.
17. Zhang, P.; Qiu, H.; Li, H.; et al. Nonmetallic Active Sites on Nickel Phosphide in Oxygen Evolution Reaction. *Nanomaterials* **2022**, *12*, 1130.
18. Perez Sirkin, Y.A.; Gadea, E.D.; Scherlis, D.A.; et al. Mechanisms of Nucleation and Stationary States of Electrochemically Generated Nanobubbles. *J. Am. Chem. Soc.* **2019**, *141*, 10801–10811.
19. Li, Q.; Liang, L.; Gerdes, K.; et al. Phase-Field Modeling of Three-Phase Electrode Microstructures in Solid Oxide Fuel Cells. *Appl. Phys. Lett.* **2012**, *101*, 033909.
20. Picardo, N. 4 Examples of Fuel Cell Modeling in COMSOL Multiphysics. Available online: https://www.comsol.com/blogs/4-examples-of-fuel-cell-modeling-in-comsol-multiphysics (accessed on 16 September 2025).
21. Ngo, S.I.; Lim, Y.I. Multiscale Eulerian CFD of Chemical Processes: A Review. *ChemEngineering* **2020**, *4*, 23.
22. Zaveri, J.; Dhanushkodi, S.R.; Fowler, M.W.; et al. Development of Deep Learning Simulation and Density Functional Theory Framework for Electrocatalyst Layers for PEM Electrolyzers. *Energies* **2025**, *18*, 1022.
23. Zhao, X.; Liu, Y. Unveiling the Active Structure of Single Nickel Atom Catalysis: Critical Roles of Charge Capacity and Hydrogen Bonding. *J. Am. Chem. Soc.* **2020**, *142*, 5773–5777.
24. Cohen, A.J.; Mori-Sánchez, P.; Yang, W. Challenges for Density Functional Theory. *Chem. Rev.* **2012**, *112*, 289–320.
25. Le, J.B.; Chen, A.; Li, L.; et al. Modeling Electrified Pt(111)-H_{ad}/Water Interfaces from Ab Initio Molecular Dynamics. *JACS Au* **2021**, *1*, 569–577.
26. Bursch, M.; Mewes, J.M.; Hansen, A.; et al. Best-Practice DFT Protocols for Basic Molecular Computational Chemistry**. *Angew. Chem. Int. Ed.* **2022**, *61*, e202205735.
27. Ju, W.; Bagger, A.; Hao, G.-P.; et al. Understanding activity and selectivity of metal-nitrogen-doped carbon catalysts for electrochemical reduction of CO_2. *Nat. Commun.* **2017**, *8*, 944.

28. Yang, H.B.; Hung, S.-F.; Liu, S.; et al. Atomically dispersed Ni(i) as the active site for electrochemical CO_2 reduction. *Nat. Energy* **2018**, *3*, 140–147.
29. Wang, A.; Li, J.; Zhang, T. Heterogeneous single-atom catalysis. *Nat. Rev. Chem.* **2018**, *2*, 65–81.
30. Kim, D.; Shi, J.; Liu, Y. Substantial Impact of Charge on Electrochemical Reactions of Two-Dimensional Materials. *J. Am. Chem. Soc.* **2018**, *140*, 9127–9131.
31. Bi, W.; Li, X.; You, R.; et al. Surface Immobilization of Transition Metal Ions on Nitrogen-Doped Graphene Realizing High-Efficient and Selective CO_2 Reduction. *Adv. Mater.* **2018**, *30*, 1706617.
32. Cheng, J.; Sprik, M. Alignment of electronic energy levels at electrochemical interfaces. *Phys. Chem. Chem. Phys.* **2012**, *14*, 11245–11267.
33. Huang, P.; Pham, T.A.; Galli, G.; et al. Alumina(0001)/Water Interface: Structural Properties and Infrared Spectra from First-Principles Molecular Dynamics Simulations. *J. Phys. Chem. C* **2014**, *118*, 8944–8951.
34. Le, J.; Iannuzzi, M.; Cuesta, A.; et al. Determining Potentials of Zero Charge of Metal Electrodes versus the Standard Hydrogen Electrode from Density-Functional-Theory-Based Molecular Dynamics. *Phys. Rev. Lett.* **2017**, *119*, 016801.
35. Cheng, J.; Sprik, M. The electric double layer at a rutile TiO_2 water interface modelled using density functional theory based molecular dynamics simulation. *J. Phys. Condens. Matter* **2014**, *26*, 244108.
36. Surendralal, S.; Todorova, M.; Finnis, M.W.; et al. First-Principles Approach to Model Electrochemical Reactions: Understanding the Fundamental Mechanisms behind Mg Corrosion. *Phys. Rev. Lett.* **2018**, *120*, 246801.
37. Lan, J.; Rybkin, V.V.; Iannuzzi, M. Ionization of Water as an Effect of Quantum Delocalization at Aqueous Electrode Interfaces. *J. Phys. Chem. Lett.* **2020**, *11*, 3724–3730.
38. Bouzid, A.; Pasquarello, A. Atomic-Scale Simulation of Electrochemical Processes at Electrode/Water Interfaces under Referenced Bias Potential. *J. Phys. Chem. Lett.* **2018**, *9*, 1880–1884.
39. Li, X.; Duan, X.; Hua, K.; et al. Local tetragonal distortion of Pt alloy catalysts for enhanced oxygen reduction reaction efficiency. *Carbon Enery* **2024**, *6*, e508.
40. Yu, C.; Xiang, Y.; Lawson, T.; et al. Graphene oxide-based nanofluidic membranes for reverse electrodialysis that generate electricity from salinity gradients. *Carbon Enery* **2024**, *7*, 626.
41. Zofchak, E.S.; Zhang, Z.; Marioni, N.; et al. Cation–polymer interactions and local heterogeneity determine the relative order of alkali cation diffusion coefficients in PEGDA hydrogels. *J. Membr. Sci.* **2023**, *685*, 121898.
42. Borodin, O.; Smith, G.D. Mechanism of Ion Transport in Amorphous Poly(ethylene oxide)/LiTFSI from Molecular Dynamics Simulations. *Macromolecules* **2006**, *39*, 1620–1629.
43. Marioni, N.; Nordness, O.; Zhang, Z.; et al. Ion and Water Dynamics in the Transition from Dry to Wet Conditions in Salt-Doped PEG. *ACS Macro Lett.* **2024**, *13*, 341–347.
44. Molinari, N.; Mailoa, J.P.; Kozinsky, B. Effect of Salt Concentration on Ion Clustering and Transport in Polymer Solid Electrolytes: A Molecular Dynamics Study of PEO–LiTFSI. *Chem. Mater.* **2018**, *30*, 6298–6306.
45. Nordness, O.; Moon, J.D.; Marioni, N.; et al. Probing Water and Ion Diffusion in Functional Hydrogel Membranes by PFG-NMR. *Macromolecules* **2023**, *56*, 4669–4680.
46. Wheatle, B.K.; Keith, J.R.; Mogurampelly, S.; et al. Influence of Dielectric Constant on Ionic Transport in Polyether-Based Electrolytes. *ACS Macro Lett.* **2017**, *6*, 1362–1367.
47. Widstrom, M.D.; Borodin, O.; Ludwig, K.B.; et al. Water Domain Enabled Transport in Polymer Electrolytes for Lithium-Ion Batteries. *Macromolecules* **2021**, *54*, 2882–2891.
48. Feng, G.; Cummings, P.T. Supercapacitor Capacitance Exhibits Oscillatory Behavior as a Function of Nanopore Size. *J. Phys. Chem. Lett.* **2011**, *2*, 2859–2864.
49. Feng, G.; Li, S.; Atchison, J.S.; et al. Molecular Insights into Carbon Nanotube Supercapacitors: Capacitance Independent of Voltage and Temperature. *J. Phys. Chem. C* **2013**, *117*, 9178–9186.
50. Hamza, M.; Mei, B.A.; Zeng, Z.; et al. Interfacial thermal signature of electrode/electrolyte interfaces and its effect on charge storage performance during charging of electrochemical energy storage devices. *Appl. Therm. Eng.* **2025**, *274*, 126660.
51. Scalfi, L.; Salanne, M.; Rotenberg, B. Molecular Simulation of Electrode-Solution Interfaces. *Annu. Rev. Phys. Chem.* **2021**, *72*, 189–212.
52. Shim, Y.; Kim, H.J.; Jung, Y. Graphene-based supercapacitors in the parallel-plate electrode configuration: Ionic liquidsversus organic electrolytes. *Faraday Discuss.* **2012**, *154*, 249–263.
53. van Duin, A.C.T.; Dasgupta, S.; Lorant, F.; et al. ReaxFF: A Reactive Force Field for Hydrocarbons. *J. Phys. Chem. A* **2001**, *105*, 9396–9409.
54. Yang, L.; Fishbine, B.H.; Migliori, A.; et al. Molecular Simulation of Electric Double-Layer Capacitors Based on Carbon Nanotube Forests. *J. Am. Chem. Soc.* **2009**, *131*, 12373–12376.
55. Yang, L.; Fishbine, B.H.; Migliori, A.; et al. Dielectric saturation of liquid propylene carbonate in electrical energy storage applications. *J. Chem. Phys.* **2010**, *132*, 044701.

56. Wang, Z.; Yang, Y.; Olmsted, D.L.; et al. Evaluation of the constant potential method in simulating electric double-layer capacitors. *J. Chem. Phys.* **2014**, *141*, 184102.
57. Holoviak, S.; Dabo, I.; Sinnott, S. Simulation of Electrochemical Oxidation in Aqueous Environments under Applied Voltage Using Classical Molecular Dynamics. *J. Phys. Chem. A* **2024**, *128*, 2236–2244.
58. Shao, M.; Chang, Q.; Dodelet, J.P.; et al. Recent Advances in Electrocatalysts for Oxygen Reduction Reaction. *Chem. Rev.* **2016**, *116*, 3594–3657.
59. Stevens, M.B.; Anand, M.; Kreider, M.E.; et al. New challenges in oxygen reduction catalysis: A consortium retrospective to inform future research. *Energy Environ. Sci.* **2022**, *15*, 3775–3794.
60. Thompson, A.P.; Aktulga, H.M.; Berger, R.; et al. LAMMPS—A flexible simulation tool for particle-based materials modeling at the atomic, meso, and continuum scales. *Comput. Phys. Commun.* **2022**, *271*, 108171.
61. Li, B.; Xiang, W.; Dou, X.; et al. Coarse-Grained Molecular Dynamics Simulation of Nucleation and Stability of Electrochemically Generated Nanobubbles. *Langmuir* **2025**, *41*, 8497–8509.
62. Ma, Y.; Guo, Z.; Chen, Q.; et al. Dynamic Equilibrium Model for Surface Nanobubbles in Electrochemistry. *Langmuir* **2021**, *37*, 2771–2779.
63. Li, B.; Ju, M.; Dou, X.; et al. Assessing nanoparticle-surfactant-salt synergistic effects on droplet–droplet electrocoalescence by molecular dynamics simulations. *J. Mol. Liq.* **2022**, *367*, 120570.
64. Lau, K.C.; Turner, C.; Dunlap, B. Kinetic Monte Carlo simulation of the Yttria Stabilized Zirconia (YSZ) fuel cell cathode. *Solid State Ion.* **2008**, *179*, 1912–1920.
65. Zhu, H.; Kee, R.J. A general mathematical model for analyzing the performance of fuel-cell membrane-electrode assemblies. *J. Power Sources* **2003**, *117*, 61–74.
66. Modak, A.; Lusk, M. Kinetic Monte Carlo simulation of a solid-oxide fuel cell: I. Open-circuit voltage and double layer structure. *Solid State Ion.* **2005**, *176*, 2181–2191.
67. Pornprasertsuk, R.; Cheng, J.; Huang, H.; et al. Electrochemical impedance analysis of solid oxide fuel cell electrolyte using kinetic Monte Carlo technique. *Solid State Ion.* **2007**, *178*, 195–205.
68. Wei, S.; Luo, Y.; Zhang, H.; et al. Voltage-Dependent Electrochemical Carbon Dioxide Reduction Mechanism Unveiled by Kinetic Monte Carlo Simulation. *J. Phys. Chem. Lett.* **2025**, *16*, 2896–2904.
69. Wu, L.; Qin, J.; Kharchenko, V.O.; et al. Phase field modeling microstructural evolution of Fe-Cr-Al systems at thermal treatment. *Front. Energy Res.* **2023**, *11*, 11:1088742.
70. Li, Q.; Xue, D.; Feng, C.; et al. Fracture Simulation of Ni–YSZ Anode Microstructures of Solid Oxide Fuel Cells Using Phase Field Method. *J. Electrochem. Soc.* **2022**, *169*, 073507.
71. Jiao, Z.; Shikazono, N. Prediction of Nickel Morphological Evolution in Composite Solid Oxide Fuel Cell Anode Using Modified Phase Field Model. *J. Electrochem. Soc.* **2018**, *165*, F55.
72. Jiao, Z.; Shikazono, N. Simulation of Nickel Morphological and Crystal Structures Evolution in Solid Oxide Fuel Cell Anode Using Phase Field Method. *J. Electrochem. Soc.* **2014**, *161*, F577.
73. Abdeljawad, F.; Völker, B.; Davis, R.; et al. Connecting microstructural coarsening processes to electrochemical performance in solid oxide fuel cells: An integrated modeling approach. *J. Power Sources* **2014**, *250*, 319–331.
74. Davis, R.; Abdeljawad, F.; Lillibridge, J.; et al. Phase wettability and microstructural evolution in solid oxide fuel cell anode materials. *Acta Mater.* **2014**, *78*, 271–281.
75. Hong, L.; Hu, J.M.; Gerdes, K.; et al. Oxygen vacancy diffusion across cathode/electrolyte interface in solid oxide fuel cells: An electrochemical phase-field model. *J. Power Sources* **2015**, *287*, 396–400.
76. Jiao, Z.; Shikazono, N. Simulation of the reduction process of solid oxide fuel cell composite anode based on phase field method. *J. Power Sources* **2016**, *305*, 10–16.
77. Kim, J.H.; Liu, W.K.; Lee, C. Multi-scale solid oxide fuel cell materials modeling. *Comput. Mech.* **2009**, *44*, 683–703.
78. Lei, Y.; Cheng, T.L.; Wen, Y.H. Phase field modeling of microstructure evolution and concomitant effective conductivity change in solid oxide fuel cell electrodes. *J. Power Sources* **2017**, *345*, 275–289.
79. Liang, L.; Li, Q.; Hu, J.; et al. Phase field modeling of microstructure evolution of electrocatalyst-infiltrated solid oxide fuel cell cathodes. *J. Appl. Phys.* **2015**, *117*, 065105.
80. Chen, L.Q. Phase-Field Models for Microstructure Evolution. *Annu. Rev. Mater. Res.* **2002**, *32*, 113–140.
81. Hong, Z.; Viswanathan, V. Open-Sourcing Phase-Field Simulations for Accelerating Energy Materials Design and Optimization. *ACS Energy Lett.* **2020**, *5*, 3254–3259.
82. Niu, Z.; Pinfield, V.J.; Wu, B.; et al. Towards the digitalisation of porous energy materials: Evolution of digital approaches for microstructural design. *Energy Environ. Sci.* **2021**, *14*, 2549–2576.
83. Valette, G. Double layer on silver single-crystal electrodes in contact with electrolytes having anions which present a slight specific adsorption: Part I. The (110) face. *J. Electroanal. Chem. Interfacial Electrochem.* **1981**, *122*, 285–297.
84. Bikerman, J.J. Structure and capacity of electrical double layer. *Lond. Edinb. Dublin Philos. Mag. J. Sci.* **2009**, *33*, 384–397.

85. Gu, J.; Liu, S.; Ni, W.; et al. Modulating electric field distribution by alkali cations for CO_2 electroreduction in strongly acidic medium. *Nat. Catal.* **2022**, *5*, 268–276.
86. Johnson, E.; Haussener, S. Contrasting Views of the Electric Double Layer in Electrochemical CO_2 Reduction: Continuum Models vs Molecular Dynamics. *J. Phys. Chem. C* **2024**, *128*, 10450–10464.
87. Kilic, M.S.; Bazant, M.Z.; Ajdari, A. Steric effects in the dynamics of electrolytes at large applied voltages. II. Modified Poisson-Nernst-Planck equations. *Phys. Rev. E* **2007**, *75*, 021503.
88. Ma, Z.; Yang, Z.; Lai, W.; et al. CO_2 electroreduction to multicarbon products in strongly acidic electrolyte via synergistically modulating the local microenvironment. *Nat. Commun.* **2022**, *13*, 7595.
89. Bohra, D.; Chaudhry, J.H.; Burdyny, T.; et al. Modeling the electrical double layer to understand the reaction environment in a CO_2 electrocatalytic system. *Energy Environ. Sci.* **2019**, *12*, 3380–3389.
90. Butt, E.N.; Padding, J.T.; Hartkamp, R. Size-modified Poisson–Nernst–Planck approach for modeling a local electrode environment in CO_2 electrolysis. *Sustain. Energy Fuels* **2023**, *7*, 144–154.
91. Johnson, E.F.; Boutin, E.; Haussener, S. Surface Charge Boundary Condition Often Misused in CO_2 Reduction Models. *J. Phys. Chem. C* **2023**, *127*, 18784–18790.
92. Johnson, E.F.; Boutin, E.; Liu, S.; et al. Pathways to enhance electrochemical CO_2 reduction identified through direct pore-level modeling. *EES Catal.* **2023**, *1*, 704–719.
93. Wang, H.; Thiele, A.; Pilon, L. Simulations of Cyclic Voltammetry for Electric Double Layers in Asymmetric Electrolytes: A Generalized Modified Poisson–Nernst–Planck Model. *J. Phys. Chem. C* **2013**, *117*, 18286–18297.
94. Govindarajan, N.; Lin, T.Y.; Roy, T.; et al. Coupling Microkinetics with Continuum Transport Models to Understand Electrochemical CO_2 Reduction in Flow Reactors. *PRX Energy* **2023**, *2*, 033010.
95. Abdulaziz, M.; Petruk, A.; Samiee, F.; et al. Advancing Hydrodynamic Electrochemistry: A Channel Flow Cell for High-Temperature and High-Pressure Applications. *J. Phys. Chem. C* **2025**, *129*, 9726–9735.
96. Forschner, L.; Artmann, E.; Jacob, T.; et al. Electric Potential Distribution Inside the Electrolyte during High Voltage Electrolysis. *J. Phys. Chem. C* **2023**, *127*, 4387–4394.
97. Moorcroft, M.J.; Lawrence, N.S.; Coles, B.A.; et al. High temperature electrochemical studies using a channel flow cell heated by radio frequency radiation. *J. Electroanal. Chem.* **2001**, *506*, 28–33.
98. Wang, H.; Jusys, Z.; Behm, R.J.; et al. A channel flow cell with double disk electrodes for oxygen electroreduction study at elevated temperatures and pressures: Theory. *J. Electroanal. Chem.* **2021**, *896*, 115251.
99. Ma, L.; Pourkashanian, M.; Carcadea, E. Review of the Computational Fluid Dynamics Modeling of Fuel Cells. *J. Fuel Cell Sci. Technol.* **2005**, *2*, 246–257.
100. Akbari, M.H.; Rismanchi, B. Numerical investigation of flow field configuration and contact resistance for PEM fuel cell performance. *Renewable Energy* **2008**, *33*, 1775–1783.
101. Kloess, J.P.; Wang, X.; Liu, J.; et al. Investigation of bio-inspired flow channel designs for bipolar plates in proton exchange membrane fuel cells. *J. Power Sources* **2009**, *188*, 132–140.
102. Liu, H.; Li, P.; Lew, J.V. CFD study on flow distribution uniformity in fuel distributors having multiple structural bifurcations of flow channels. *Int. J. Hydrogen Energy* **2010**, *35*, 9186–9198.
103. Sierra, J.M.; Figueroa-Ramírez, S.J.; Díaz, S.E.; et al. Numerical evaluation of a PEM fuel cell with conventional flow fields adapted to tubular plates. *Int. J. Hydrogen Energy* **2014**, *39*, 16694–16705.
104. Um, S.; Wang, C.Y. Three-dimensional analysis of transport and electrochemical reactions in polymer electrolyte fuel cells. *J. Power Sources* **2004**, *125*, 40–51.
105. Vazifeshenas, Y.; Sedighi, K.; Shakeri, M. Numerical investigation of a novel compound flow-field for PEMFC performance improvement. *Int. J. Hydrogen Energy* **2015**, *40*, 15032–15039.
106. Wilberforce, T.; El-Hassan, Z.; Khatib, F.N.; et al. Development of Bi-polar plate design of PEM fuel cell using CFD techniques. *Int. J. Hydrogen Energy* **2017**, *42*, 25663–25685.
107. Wilberforce, T.; Ijaodola, O.; Emmanuel, O.; et al. Optimization of Fuel Cell Performance Using Computational Fluid Dynamics. *Membranes* **2021**, *11*, 146.
108. García, M.; Izquierdo, S.; Fueyo, N. Challenges in the electrochemical modelling of solid oxide fuel and electrolyser cells. *Renew. Sustain. Energy Rev.* **2014**, *33*, 701–718.
109. Hess, B.; Kutzner, C.; van der Spoel, D.; et al. GROMACS 4: Algorithms for Highly Efficient, Load-Balanced, and Scalable Molecular Simulation. *J. Chem. Theory Comput.* **2008**, *4*, 435–447.
110. Bekas, C.; Curioni, A. Very large scale wavefunction orthogonalization in Density Functional Theory electronic structure calculations. *Comput. Phys. Commun.* **2010**, *181*, 1057–1068.
111. Fermeglia, M.; Pricl, S. Multiscale molecular modeling in nanostructured material design and process system engineering. *Comput. Chem. Eng.* **2009**, *33*, 1701–1710.
112. Olsen, J.M.H.; Bolnykh, V.; Meloni, S.; et al. MiMiC: A Novel Framework for Multiscale Modeling in Computational Chemistry. *J. Chem. Theory Comput.* **2019**, *15*, 3810–3823.

113. Phillips, J.C.; Sun, Y.; Jain, N.; et al. Mapping to Irregular Torus Topologies and Other Techniques for Petascale Biomolecular Simulation. In Proceedings of the International Conference for High Performance Computing, Networking, Storage and Analysis, New Orleans, LA, USA,16–21 November 2014; pp. 81–91.
114. Salomon-Ferrer, R.; Götz, A.W.; Poole, D.; et al. Routine Microsecond Molecular Dynamics Simulations with AMBER on GPUs. 2. Explicit Solvent Particle Mesh Ewald. *J. Chem. Theory Comput.* **2013**, *9*, 3878–3888.
115. VandeVondele, J.; Krack, M.; Mohamed, F.; et al. Quickstep: Fast and accurate density functional calculations using a mixed Gaussian and plane waves approach. *Comput. Phys. Commun.* **2005**, *167*, 103–128.
116. AIP Publishing LLC. *Multiscale Modeling of Electrochemical Reactions and Processes*; AIP Publishing LLC: Melville, NY, USA, 2021. https://doi.org/10.1063/9780735422377.
117. Singharoy, A.; Joshi, H.; Ortoleva, P.J. Multiscale Macromolecular Simulation: Role of Evolving Ensembles. *J. Chem. Inf. Model.* **2012**, *52*, 2638–2649.
118. Delgado-Buscalioni, R.; Coveney, P.V.; Riley, G.D.; et al. Hybrid molecular-continuum fluid models: Implementation within a general coupling framework. *Philos. Trans. R. Soc. A Math. Phys. Eng. Sci.* **2005**, *363*, 1975–1985.
119. Ingólfsson, H.I.; Bhatia, H.; Aydin, F.; et al. Machine Learning-Driven Multiscale Modeling: Bridging the Scales with a Next-Generation Simulation Infrastructure. *J. Chem. Theory Comput.* **2023**, *19*, 2658–2675.
120. Vlachos, D.G. Multiscale modeling for emergent behavior, complexity, and combinatorial explosion. *AlChE J.* **2012**, *58*, 1314–1325.
121. Zhang, Y.; Liu, H.; Yang, W. Free energy calculation on enzyme reactions with an efficient iterative procedure to determine minimum energy paths on a combined ab initio QM/MM potential energy surface. *J. Chem. Phys.* **2000**, *112*, 3483–3492.
122. Zuckerman, D.M.; Chong, L.T. Weighted Ensemble Simulation: Review of Methodology, Applications, and Software. *Annu. Rev. Biophys.* **2017**, *46*, 43–57.
123. Bernstein, N.; Várnai, C.; Solt, I.; et al. QM/MM simulation of liquid water with an adaptive quantum region. *Phys. Chem. Chem. Phys.* **2012**, *14*, 646–656.
124. Dapprich, S.; Komaromi, I.; Byun, K.S.; et al. A new ONIOM implementation in Gaussian98. Part I. The calculation of energies, gradients, vibrational frequencies and electric field derivatives. *J. Mol. Struct.* **1999**, *461–462*, 1–21.
125. Heyden, A.; Lin, H.; Truhlar, D.G. Adaptive Partitioning in Combined Quantum Mechanical and Molecular Mechanical Calculations of Potential Energy Functions for Multiscale Simulations. *J. Phys. Chem. B* **2007**, *111*, 2231–2241.
126. Rowley, C.N.; Roux, B. The Solvation Structure of Na^+ and K^+ in Liquid Water Determined from High Level ab Initio Molecular Dynamics Simulations. *J. Chem. Theory Comput.* **2012**, *8*, 3526–3535.
127. Takahashi, H.; Kambe, H.; Morita, A. A simple and effective solution to the constrained QM/MM simulations. *J. Chem. Phys.* **2018**, *148*, 134119.
128. Takenaka, N.; Kitamura, Y.; Koyano, Y.; et al. The number-adaptive multiscale QM/MM molecular dynamics simulation: Application to liquid water. *Chem. Phys. Lett.* **2012**, *524*, 56–61.
129. Tzeliou, C.E.; Mermigki, M.A.; Tzeli, D. Review on the QM/MM Methodologies and Their Application to Metalloproteins. *Molecules* **2022**, *27*, 2660.
130. Vreven, T.; Morokuma, K. *Chapter 3 Hybrid Methods: ONIOM(QM:MM) and QM/MM*; Elsevier: Amsterdam, The Netherlands, 2006; pp. 35–51.
131. Watanabe, H.C.; Kubař, T.; Elstner, M. Size-Consistent Multipartitioning QM/MM: A Stable and Efficient Adaptive QM/MM Method. *J. Chem. Theory Comput.* **2014**, *10*, 4242–4252.
132. Zhang, R.; Lev, B.; Cuervo, J.E.; et al. A Guide to QM/MM Methodology and Applications. *Adv. Quantum Chem.* **2010**, *59*, 353–400.
133. Mihai, D.P.; Nitulescu, G.M. Computer-Aided Drug Design and Drug Discovery. *Pharmaceuticals* **2025**, *18*, 436.
134. Jaramillo, T.F.; Jørgensen, K.P.; Bonde, J.; et al. Identification of Active Edge Sites for Electrochemical H_2 Evolution from MoS_2 Nanocatalysts. *Science* **2007**, *317*, 100–102.
135. Bawari, S.; Narayanan, T.N.; Mondal, J. Atomistic Elucidation of Sorption Processes in Hydrogen Evolution Reaction on a van der Waals Heterostructure. *J. Phys. Chem. C* **2018**, *122*, 10034–10041.
136. Chen, L.; Zhang, X.; Chen, A.; et al. Targeted design of advanced electrocatalysts by machine learning. *Chin. J. Catal.* **2022**, *43*, 11–32.
137. Du, C.; Qiu, C.; Fang, Z.; et al. Interface hydrophobic tunnel engineering: A general strategy to boost electrochemical conversion of N_2 to NH_3. *Nano Energy* **2022**, *92*, 106784.
138. Hu, X.; Chen, S.; Chen, L.; et al. What is the Real Origin of the Activity of Fe–N–C Electrocatalysts in the O_2 Reduction Reaction? Critical Roles of Coordinating Pyrrolic N and Axially Adsorbing Species. *J. Am. Chem. Soc.* **2022**, *144*, 18144–18152.
139. Wang, X.; Zhu, J.; Kuang, Y.; et al. pH-dependent formation potential of OH* on Pt(111): Double layer effect on water dissociation. *Nano Mater. Sci.* **2025**, *7*, 493–499.

140. Menezes, P.W.; Indra, A.; Das, C.; et al. Uncovering the Nature of Active Species of Nickel Phosphide Catalysts in High-Performance Electrochemical Overall Water Splitting. *ACS Catal.* **2016**, *7*, 103–109.
141. Nørskov, J.K.; Bligaard, T.; Hvolbæk, B.; et al. The nature of the active site in heterogeneous metal catalysis. *Chem. Soc. Rev.* **2008**, *37*, 2163–2171.
142. Rossmeisl, J.; Logadottir, A.; Nørskov, J.K. Electrolysis of water on (oxidized) metal surfaces. *Chem. Phys.* **2005**, *319*, 178–184.
143. Seh, Z.W.; Kibsgaard, J.; Dickens, C.F.; et al. Combining theory and experiment in electrocatalysis: Insights into materials design. *Science* **2017**, *355*, eaad4998.
144. Stern, L.A.; Feng, L.; Song, F.; et al. Ni_2P as a Janus catalyst for water splitting: The oxygen evolution activity of Ni_2P nanoparticles. *Energy Environ. Sci.* **2015**, *8*, 2347–2351.
145. Verma, A.K.; Verma, A.M.; Govind Rajan, A. Theoretical understanding of electrochemical phenomena in 2D electrode materials. *Curr. Opin. Electrochem.* **2022**, *36*, 101116.
146. Wang, Y.; Shao, H.; Zhang, C.; et al. Molecular dynamics for electrocatalysis: Mechanism explanation and performance prediction. *Energy Rev.* **2023**, *2*, 100028.
147. Wang, Y.; Su, H.; He, Y.; et al. Advanced Electrocatalysts with Single-Metal-Atom Active Sites. *Chem. Rev.* **2020**, *120*, 12217–12314.
148. Wen, S.; Chen, G.; Chen, W.; et al. Nb-doped layered FeNi phosphide nanosheets for highly efficient overall water splitting under high current densities. *J. Mater. Chem. A* **2021**, *9*, 9918–9926.
149. Xue, Y.; Guo, Y.; Cui, H.; et al. Catalyst Design for Electrochemical Reduction of CO2 to Multicarbon Products. *Small Methods* **2021**, *5*, 2100736.
150. Cheng, Q.; Wang, M.; Ni, J.; et al. Comprehensive understanding and rational regulation of microenvironment for gas-involving electrochemical reactions. *Carbon Enery* **2023**, *5*, e307.
151. Zhang, X.; Wang, J.; Zong, K.; et al. Recent advances in non-noble metal-based electrocatalysts for hybrid water electrolysis systems. *Carbon Energy* **2025**, *7*, e679.
152. Chen, Q.; Luo, L.; White, H.S. Electrochemical Generation of a Hydrogen Bubble at a Recessed Platinum Nanopore Electrode. *Langmuir* **2015**, *31*, 4573–4581.
153. German, S.R.; Edwards, M.A.; Chen, Q.; et al. Electrochemistry of single nanobubbles. Estimating the critical size of bubble-forming nuclei for gas-evolving electrode reactions. *Faraday Discuss.* **2016**, *193*, 223–240.
154. Gupta, S.; Patel, N.; Fernandes, R.; et al. Co–Ni–B nanocatalyst for efficient hydrogen evolution reaction in wide pH range. *Appl. Catal. B Environ.* **2016**, *192*, 126–133.
155. Luo, L.; White, H.S. Electrogeneration of Single Nanobubbles at Sub-50-nm-Radius Platinum Nanodisk Electrodes. *Langmuir* **2013**, *29*, 11169–11175.
156. Mao, S.; Wen, Z.; Huang, T.; et al. High-performance bi-functional electrocatalysts of 3D crumpled graphene–cobalt oxide nanohybrids for oxygen reduction and evolution reactions. *Energy Environ. Sci.* **2014**, *7*, 609–616.
157. Mazloomi, S.K.; Sulaiman, N. Influencing factors of water electrolysis electrical efficiency. *Renew. Sustain. Energy Rev.* **2012**, *16*, 4257–4263.
158. Zhang, L.; Zhang, Y.; Zhang, X.; et al. Electrochemically Controlled Formation and Growth of Hydrogen Nanobubbles. *Langmuir* **2006**, *22*, 8109–8113.
159. Zhang, C.; Hu, K.; Liu, X.; et al. Unraveling the Influence of Nafion Content on the Performance of Proton-Exchange Membrane Fuel Cells from the Perspective of Triple-Phase Boundary. *Langmuir* **2024**, *40*, 15520–15529.
160. Di Noto, V.; Piga, M.; Giffin, G.A.; et al. Interplay between Mechanical, Electrical, and Thermal Relaxations in Nanocomposite Proton Conducting Membranes Based on Nafion and a $[(ZrO_2)\cdot(Ta_2O_5)0.119]$ Core–Shell Nanofiller. *J. Am. Chem. Soc.* **2012**, *134*, 19099–19107.
161. Vezzù, K.; Maes, A.M.; Bertasi, F.; et al. Interplay Between Hydroxyl Density and Relaxations in Poly(vinylbenzyltrime thylammonium)-b-poly(methylbutylene) Membranes for Electrochemical Applications. *J. Am. Chem. Soc.* **2018**, *140*, 1372–1384.
162. Vezzù, K.; Nawn, G.; Negro, E.; et al. Electric Response and Conductivity Mechanism of Blended Polyvinylidene Fluoride/Nafion Electrospun Nanofibers. *J. Am. Chem. Soc.* **2019**, *142*, 801–814.
163. Wang, Z.; Sun, G.; Lewis, N.H.C.; et al. Water-mediated ion transport in an anion exchange membrane. *Nat. Commun.* **2025**, *16*, 1099.
164. Gao, M.R.; Zhu, M.N.; Zhang, B.W.; et al. Strategic Design of "Thre-in-One" Cathode Toward Optimal Performance of Proton-Conducting Solid Oxide Fuel Cell: The Temperature Matters. *Carbon Enery* **2025**, *7*, e683.
165. Wu, Z.; Zhu, P.; Huang, Y.; et al. A Comprehensive Review of Modeling of Solid Oxide Fuel Cells: From Large Systems to Fine Electrodes. *Chem. Rev.* **2025**, *125*, 2184–2268.
166. Lian, C.; Janssen, M.; Liu, H.; et al. Blessing and Curse: How a Supercapacitor's Large Capacitance Causes its Slow Charging. *Phys. Rev. Lett.* **2020**, *124*, 076001.

167. Lin, Y.; Lian, C.; Berrueta, M.U.; et al. Microscopic Model for Cyclic Voltammetry of Porous Electrodes. *Phys. Rev. Lett.* **2022**, *128*, 206001.
168. Bosio, B.; Bianchi, F.R. Multiscale modelling potentialities for solid oxide fuel cell performance and degradation analysis. *Sustain. Energy Fuels* **2023**, *7*, 280–293.
169. Bramley, G.A.; Beynon, O.T.; Stishenko, P.V.; et al. The application of QM/MM simulations in heterogeneous catalysis. *Phys. Chem. Chem. Phys.* **2023**, *25*, 6562–6585.
170. Deng, Z.; Kumar, V.; Bölle, F.T.; et al. Towards autonomous high-throughput multiscale modelling of battery interfaces. *Energy Environ. Sci.* **2022**, *15*, 579–594.
171. Ding, R.; Chen, J.; Chen, Y.; et al. Unlocking the potential: Machine learning applications in electrocatalyst design for electrochemical hydrogen energy transformation. *Chem. Soc. Rev.* **2024**, *53*, 11390–11461.
172. Elliott, J.D.; Papaderakis, A.A.; Dryfe, R.A.W.; et al. The electrochemical double layer at the graphene/aqueous electrolyte interface: What we can learn from simulations, experiments, and theory. *J. Mater. Chem. C* **2022**, *10*, 15225–15262.
173. Kovalenko, A.; Gusarov, S. Multiscale methods framework: Self-consistent coupling of molecular theory of solvation with quantum chemistry, molecular simulations, and dissipative particle dynamics. *Phys. Chem. Chem. Phys.* **2018**, *20*, 2947–2969.
174. Li, Q.; Ouyang, Y.; Lu, S.; et al. Perspective on theoretical methods and modeling relating to electro-catalysis processes. *Chem. Commun.* **2020**, *56*, 9937–9949.
175. Senthilnathan, D.; Giunta, P.; Vetere, V.; et al. An efficient and cyclic hydrogen evolution reaction mechanism on $[Ni(PH_2NH_2)_2]^{2+}$ catalysts: A theoretical and multiscale simulation study. *RSC Adv.* **2014**, *4*, 5177–5187.
176. Gong, H.; Sun, G.; Shi, W.; et al. Nano-Au-decorated hierarchical porous cobalt sulfide derived from ZIF-67 toward optimized oxygen evolution catalysis: Important roles of microstructures and electronic modulation. *Carbon Enery* **2024**, *6*, e432.
177. Yuan, Y.; Zheng, Y.; Luo, D.; et al. Recent progress on mechanisms, principles, and strategies for high-activity and high-stability non-PGM fuel cell catalyst design. *Carbon Enery* **2024**, *6*, e462.
178. Back, S.; Tran, K.; Ulissi, Z.W. Toward a Design of Active Oxygen Evolution Catalysts: Insights from Automated Density Functional Theory Calculations and Machine Learning. *ACS Catal.* **2019**, *9*, 7651–7659.
179. Mou, T.; Pillai, H.S.; Wang, S.; et al. Bridging the complexity gap in computational heterogeneous catalysis with machine learning. *Nat. Catal.* **2023**, *6*, 122–136.
180. Fung, V.; Hu, G.; Ganesh, P.; et al. Machine learned features from density of states for accurate adsorption energy prediction. *Nat. Commun.* **2021**, *12*, 88.
181. Shang, Z.; Li, H. Distribution of Oxygen Vacancies in RuO2 Catalysts and Their Roles in Activity and Stability in Acidic Oxygen Evolution Reaction. *J. Phys. Chem. Lett.* **2025**, *16*, 5418–5428.
182. Shang, Z.; Zhao, S.; Dang, Q.; et al. A General Machine-Learning Framework for High-Throughput Screening for Stable and Efficient RuO_2-Based Acidic Oxygen Evolution Reaction Catalysts. *ACS Catal.* **2025**, *15*, 12835–12847.
183. Takahashi, T.; Ikeda, T.; Murata, K.; et al. Accelerated Durability Testing of Fuel Cell Stacks for Commercial Automotive Applications: A Case Study. *J. Electrochem. Soc.* **2022**, *169*, 044523.
184. Wang, Y.; Seo, B.; Wang, B.; et al. Fundamentals, materials, and machine learning of polymer electrolyte membrane fuel cell technology. *Energy AI* **2020**, *1*, 100014.
185. Yin, P.; Niu, X.; Li, S.-B.; et al. Machine-learning-accelerated design of high-performance platinum intermetallic nanoparticle fuel cell catalysts. *Nat. Commun.* **2024**, *15*, 10.
186. Zhong, M.; Tran, K.; Min, Y.; et al. Accelerated discovery of CO2 electrocatalysts using active machine learning. *Nature* **2020**, *581*, 178–183.
187. Konno, N.; Mizuno, S.; Nakaji, H.; et al. Development of Compact and High-Performance Fuel Cell Stack. *SAE Int. J. Alt. Power.* **2015**, *4*, 123–129.
188. Xu, H.; Cheng, D.; Cao, D.; et al. Revisiting the universal principle for the rational design of single-atom electrocatalysts. *Nat. Catal.* **2024**, *7*, 207–218.
189. Choubisa, H.; Abed, J.; Mendoza, D.; et al. Accelerated chemical space search using a quantum-inspired cluster expansion approach. *Matter* **2023**, *6*, 605–625.
190. Jia, Y.; Zhang, R.; Fang, C.; et al. Interpretable Machine Learning To Accelerate the Analysis of Doping Effect on Li/Ni Exchange in Ni-Rich Layered Oxide Cathodes. *J. Phys. Chem. Lett.* **2024**, *15*, 1765–1773.
191. Ma, N.; Zhang, Y.; Wang, Y.; et al. Machine learning-assisted exploration of the intrinsic factors affecting the catalytic activity of ORR/OER bifunctional catalysts. *Appl. Surf. Sci.* **2023**, *628*, 157225.
192. Mamun, O.; Winther, K.T.; Boes, J.R.; et al. A Bayesian framework for adsorption energy prediction on bimetallic alloy catalysts. *NPJ Comput. Mater.* **2020**, *6*, 177.
193. O'Connor, N.J.; Jonayat, A.S.M.; Janik, M.J.; et al. Interaction trends between single metal atoms and oxide supports identified with density functional theory and statistical learning. *Nat. Catal.* **2018**, *1*, 531–539.

194. Andersen, M.; Levchenko, S.V.; Scheffler, M.; et al. Beyond Scaling Relations for the Description of Catalytic Materials. *ACS Catal.* **2019**, *9*, 2752–2759.
195. Back, S.; Yoon, J.; Tian, N.; et al. Convolutional Neural Network of Atomic Surface Structures To Predict Binding Energies for High-Throughput Screening of Catalysts. *J. Phys. Chem. Lett.* **2019**, *10*, 4401–4408.
196. Chen, C.; Ye, W.; Zuo, Y.; et al. Graph Networks as a Universal Machine Learning Framework for Molecules and Crystals. *Chem. Mater.* **2019**, *31*, 3564–3572.
197. Chen, C.; Zuo, Y.; Ye, W.; et al. A Critical Review of Machine Learning of Energy Materials. *Adv. Energy Mater.* **2020**, *10*, 1903242.
198. Chen, D.; Shang, C.; Liu, Z.P. Machine-learning atomic simulation for heterogeneous catalysis. *NPJ Comput. Mater.* **2023**, *9*, 2.
199. Fung, V.; Hu, G.; Sumpter, B. Electronic band contraction induced low temperature methane activation on metal alloys. *J. Mater. Chem. A* **2020**, *8*, 6057–6066.
200. Goldsmith, B.R.; Esterhuizen, J.; Liu, J.X.; et al. Machine learning for heterogeneous catalyst design and discovery. *AIChE J.* **2018**, *64*, 2311–2323.
201. Gu, G.H.; Choi, C.; Lee, Y.; et al. Progress in Computational and Machine-Learning Methods for Heterogeneous Small-Molecule Activation. *Adv. Mater.* **2020**, *32*, 1907865.
202. Wang, S.; Li, Y.; Dai, S.; et al. Prediction by Convolutional Neural Networks of CO2/N2 Selectivity in Porous Carbons from N2 Adsorption Isotherm at 77 K. *Angew. Chem. Int. Ed.* **2020**, *59*, 19645–19648.
203. Xie, T.; Grossman, J.C. Crystal Graph Convolutional Neural Networks for an Accurate and Interpretable Prediction of Material Properties. *Phys. Rev. Lett.* **2018**, *120*, 145301.
204. Wang, Y.; Meyer, Q.; Tang, K.; et al. Large-scale physically accurate modelling of real proton exchange membrane fuel cell with deep learning. *Nat. Commun.* **2023**, *14*, 745.
205. Niu, Y.; Heydari, A.; Qiu, W.; et al. Machine learning-enabled performance prediction and optimization for iron–chromium redox flow batteries. *Nanoscale* **2024**, *16*, 3994–4003.
206. Wu, Z.; Chen, F.; Zhou, Z.; et al. Data-driven macro-scale simulation for rapid electrolyte wetting in lithium-ion batteries. *J. Energy Storage* **2025**, *106*, 114704.
207. Xu, C.; Li, K.; Liu, S.; et al. Identification of Cu-N2 Sites for Zn-Air Batteries in Harsh Electrolytes: Computer Virtual Screening, Machine Learning, and Practical Application. *CCS Chem.* **2025**, 1–15. https://doi.org/10.31635/ccschem.025.202505577
208. Aykol, M.; Herring, P.; Anapolsky, A. Machine learning for continuous innovation in battery technologies. *Nat. Rev. Mater.* **2020**, *5*, 725–727.
209. Kim, S.C.; Oyakhire, S.T.; Athanitis, C.; et al. Data-driven electrolyte design for lithium metal anodes. *Proc. Natl. Acad. Sci. USA* **2023**, *120*, e2214357120.
210. Makki Abadi, M.; Rashidi, M.M. Machine Learning for the Optimization and Performance Prediction of Solid Oxide Electrolysis Cells: A Review. *Processes* **2025**, *13*, 875.
211. Aldoseri, A.; Al-Khalifa, K.N.; Hamouda, A.M. Re-Thinking Data Strategy and Integration for Artificial Intelligence: Concepts, Opportunities, and Challenges. *Appl. Sci.* **2023**, *13*, 7082.
212. Sendek, A.D.; Cubuk, E.D.; Antoniuk, E.R.; et al. Machine Learning-Assisted Discovery of Solid Li-Ion Conducting Materials. *Chem. Mater.* **2018**, *31*, 342–352.
213. Yu, H.; Zhang, L.; Wang, W.; et al. Lithium-ion battery multi-scale modeling coupled with simplified electrochemical model and kinetic Monte Carlo model. *iScience* **2023**, *26*, 107661.
214. Tao, H.; Wang, S.; Liu, H.; et al. Deep Neural Network Enhanced Mesoscopic Thermodynamic Model for Unlocking the Electrode/Electrolyte Interface. *Angew. Chem. Int. Ed.* **2025**, *64*, e202418447.
215. Huang, P.; Leng, Y.; Lian, C.; et al. Porous-DeepONet: Learning the Solution Operators of Parametric Reactive Transport Equations in Porous Media. *Engineering* **2024**, *39*, 101–111.
216. Zhu, Q.; Huang, Y.; Zhou, D.; et al. Automated synthesis of oxygen-producing catalysts from Martian meteorites by a robotic AI chemist. *Nat. Synth.* **2024**, *3*, 319–328.
217. Fu, R.; Wang, L.; Yang, X.; et al. Defects-Engineered Metal-Organic Frameworksfor Supercapacitor Platform. *Sustain. Eng. Novit* **2025**, *1*, 2.
218. Song, X.; Ge, Y,; Xue, X.; et al. Electrolyte-triggered in-situ polymerization of multi-site organic cathodes for superior-longevity cation-anion co-storage secondary batteries. *Chem. Eng. J.* **2024**, *499*, 156359.
219. Zhou, X.; Wang, Y.; Gu, Y.; et al. All-Purpose Redox-Active Metal–Organic Frameworks as Both Cathodic and Anodic Host Materials for Advanced Lithium-Sulfur Batteries. *Matter* **2024**, *7*, 3069–3082.
220. Liu, S.; Tian, B.; Wang, X.; et al. The Critical Role of Initial/Operando Oxygen Loading in General Bismuth-Based Catalysts for Electroreduction of Carbon Dioxide. *J. Phys. Chem. Lett.* **2022**, *13*, 9607–9617.